UNIVERSITY OF OKLAHOMA

GRADUATE COLLEGE

Long Term Evolution – License Assisted Access (LTE-LAA): Modeling and Coexistence Performance Analysis

A DISSERTATION

SUBMITTED TO THE GRADUATE FACULTY

in partial fulfillment of the requirements for the

Degree of

DOCTOR OF PHILOSOPHY
(Ph.D)

in
Electrical and Computer Engineering

By

Naim Bitar
Norman, Oklahoma
2019

LONG TERM EVOLUTION - LICENSE ASSISTED ACCESS (LTE-LAA):
MODELING AND COEXISTENCE PERFORMANCE ANALYSIS

A DISSERTATION APPROVED FOR THE
SCHOOL OF ELECTRICAL AND COMPUTER ENGINEERING

BY

Dr. Hazem H. Refai, Chair

Dr. Curt Adams

Dr. James J. Sluss, Jr.

Dr. Thordur Runolfsson

Dr. Ali Imran

To my wife, the Love of my life, Christen Bitar,

To my parents, Samira and George.

To my sister, Alfreda.

I dedicate this humble work to you all.

Acknowledgements

I would like to sincerely thank my advisor, Prof. Hazem Refai for his continuous support, guidance and dedication throughout my time at OU. He encouraged me to keep developing my research skills and continually motivated my analytical thinking. In addition, I am very grateful to my doctoral committee and wish to thank Dr. Curt Adams, Dr. James Sluss, Dr. Thordur Runolfsson and Dr. Ali Imran for their support and advice. I also wish to express my gratitude to the OU family of professors, students and staff. My sincere appreciation to you all.

Contents

List of Figures

List of Tables

Abstract

Wireless communication built upon radio spectrum plays an instrumental role in today's modern world. With the explosive growth of mobile data traffic, mobile cellular networks need more spectrum to boost their system capacity. Long Term Evolution (LTE) technology leveraging the unlicensed band is anticipated to provide a solution to address this challenge. However, ensuring fair operation in terms of spectrum sharing with current unlicensed spectrum incumbents remains a key challenge for the success and viability of Unlicensed LTE (U-LTE). In particular, fair co-existence between unlicensed LTE and the Institute of Electrical and Electronics Engineers (IEEE) 802.11x standard, known as Wi-Fi, remains a principal concern, due to the ubiquitous, high-throughput and high capacity nature of both technologies.

This work addresses the problem of modeling and evaluating the coexistence of LTE License-Assisted-Access (LTE-LAA) in the unlicensed band. The research work presents a novel analytical model using Markov Chain to accurately model the LAA Listen-Before-Talk (LBT) scheme, as specified in the final technical specification 36.213 of the 3rd Generation Partnership Project (3GPP) release 13 and 14. Model validation is demonstrated through numerical and simulation result comparison. Model performance evaluation is examined and contrasted with the IEEE 802.11 Distributed Coordination Function (DCF) and analysis results are subsequently presented and discussed herein. Finally, succeeding model de-

velopment, a comprehensive coexistence performance analysis study is developed and completed examining the coexistence of homogeneous and heterogeneous network scenarios consisting of LTE-LAA and Wi-Fi nodes. As a result, the contribution of this work establishes a novel apparatus that facilitates numerical analysis of the LTE-LAA LBT mechanism and enables numerical comparison of future enhancements with the standardized LTE-LAA framework. In addition, this work delivers a delineating, unequivocal and in-depth examination of the effects and implications that the LTE-LAA LBT mechanism and its parameters have on coexistence performance of homogeneous and heterogeneous co-channel and co-located networks.

Chapter 1

Introduction

It is predicted that global mobile data traffic will increase to nearly 7-fold between 2016 - 2021, reaching a staggering 49 exabytes per month by 2021. [1]. This is due to the ever changing mix and growth of wireless devices that are accessing mobile networks worldwide. Compounded by the advent of ubiquitous Internet of Things (IoT) communications, the continually growing number of wireless users, new devices in different form factors with increased capabilities and intelligence, and an increasing number and variety of demanding communication services all continually being introduced in the market. As a result, the challenge of delivering and guaranteeing an adequate level of Quality of service (QoS) has increased several folds. Consequently, high capacity networks and service provisioning of very high data rates has become an essential requisite needed to meet customers' expectations. Addressing this challenge has been the focus of wireless researchers for many years now [2–5]. Nevertheless, a common opinion shared amongst the various solutions proposed is that more spectrum is needed for cellular operators to meet the anticipated continually increasing demand [6–8].

1.1 Motivation

Given the presence of substantial blocks of spectrum resources assigned or planned to be assigned in the unlicensed band, the spectrum scarcity challenge facing mobile operators can be greatly alleviated by exploiting the unlicensed spectrum. Accordingly, Unlicensed Long-Term Evolution (U-LTE) has emerged as a leading candidate solution that is anticipated to address the spectrum scarcity challenge. However, unlike the licensed spectrum, the unlicensed band is open resource, and therefore can be used by anyone as long as the basic constraints of transmit power spectral density are satisfied. Consequently, a critical element in the design of LTE in the unlicensed band rests on ensuring it can operate fairly, in terms of spectrum sharing, with other unlicensed spectrum incumbents. This has been proven to be a challenging and critical mandate for the success of U-LTE. To address this issue, a number of mechanisms have been proposed and developed that modify LTE and make it more amenable to coexist with other wireless technologies. These mechanisms include LTE Unlicensed (LTE-U), Licensed-Assisted-Access (LAA), enhanced-LAA (eLAA), LTE Wireless Local Area Network Aggregation (LTE-WLAN) also known as (LWA), and Multefire. During the development of these technologies, initial experimentation work assessing their effects on the performance of 802.11 incumbent wireless networks utilizing the same unlicensed band, mainly carried out by commercial operators, indicated minor impact [9–12]. Other experiments, carried out by the research community, indicated that the performance of Wi-Fi would be seriously affected, all while the performance of LTE would only be slightly degraded [13–15]. This discordant outcome could be attributed to discrepancies in the experimentation tools implementing the LTE unlicensed specifications. Furthermore, industry results

based on simulations or empirical experiments remain independently unverifiable (as they rely on proprietary tools and resources) and lack an analytical basis that accords the necessary research transparency. This impasse of dueling positions signifies the imperative necessity of an analytical modeling framework to be considered for analyzing and evaluating the proposed specifications. This would allow accurate transparent analytical assessment of the underlying mechanisms while eliminating implementation biases that could arise in empirical experimentation.

1.2 Contribution

This research work builds upon the desired mathematical framework. It addresses the issue of evaluating and modeling LTE-LAA's Listen-Before-Talk (LBT) mechanism and its effect on the coexistence of the technology in the unlicensed band. The work begins by reviewing candidate coexistence solutions for Unlicensed LTE that have been proposed, developed and standardized as of date. Then, the work presents a novel analytical model using Markov Chain that accurately models the 3GPP LTE-LAA LBT scheme, as specified in the final 3rd Generation Partnership Project (3GPP) standard for LAA which has been additionally adopted in the Multefire specification as well. Model validation is demonstrated through numerical and simulation result comparison and performance evaluation is conducted between the LAA-LBT and the Institute of Electrical and Electronics Engineers (IEEE) 802.11 Distributed Coordination Function (DCF). Furthermore, following model development, a comprehensive coexistence analysis study of both homogeneous and heterogeneous network scenarios involving LTE-LAA Evolved Node Bs (eNB) and Wi-Fi Access Points (APs) is carried out. Results

are subsequently presented and discussed herein.

The investigations of this dissertation have produced the following contributions to our field:

1. The work establishes a novel and accurate analytical model that enables numerical analysis of the LTE-LAA coexistence mechanism as defined in the final standardized technical specification (TS) 36.213 of 3GPP release 13 and 14. This is in response to the need for a mathematical framework that facilities coexistence performance analysis of the newly standardized technology, aiding in the early evaluation and understanding of the technology performance, taking into account the lack of any commercial or open source tools or equipment that implement the standard as of date. Furthermore, the developed model enables future modifications and enhancements to be contrasted with the current standardized LTE-LAA LBT framework.

2. The work expounds the LTE-LAA LBT and delineates the effects of the standardized coexistence mechanism and its newly introduced operational parameter and their interactions through a detailed examination. The outcome of this provides an unequivocal and clear understanding of the implications and effects on the coexistence mechanism performance.

3. The work details a comprehensive coexistence analysis study completed for both homogeneous and heterogeneous networks, clearly identifying when the LTE-LAA LBT mechanism will obtain increased performance gain over co-channel incumbents and the effects on both co-channel and co-located networks.

The balance of this dissertation is organized as follows: The following section presents the background and related work exposition on LTE coexistence in the

unlicensed band. Chapter 2 provides a brief overview of the unlicensed band regulations, the 802.11 standard, and the candidate coexistence solutions that have been standardized. Chapter 3 presents the proposed analytical model of LTE-LAA LBT, demonstrates validation work through numerical and simulation analysis and presents a performance evaluation of LAA-LBT by means of the proposed model contrasted with the 802.11 DCF. Chapter 4 presents a coexistence performance analysis of both homogeneous and heterogeneous networks consisting of LTE-LAA eNB nodes and WiFi APs. Finally, chapter 5 concludes the dissertation.

1.3 Background and Related Work

With the initial consideration of permitting licensed LTE to supplement its downlink with unlicensed spectrum, various early experimentation work clearly indicated that the established LTE technology would unfairly occupy the unlicensed-band and induce adverse effects on current unlicensed-band occupants [16–18]. This impelled research to ensue in attempt to address the challenge of coexistence. However, with two distinct global-market regulatory constraints i.e. (regions having no LBT restriction, and other regions requiring LBT), two distinct research directions developed: The first direction matured into what is now termed LTE-U. This position assumes no LBT constraint and is currently adopted by the LTE-U Forum [19]. This approach can readily apply 3GPP release 10, 11 & 12 enhancements coupling them with coexistence methods that monitor band occupancy and attempt to replicate channel retention/idle time in their resource allocation mechanisms through duty cycling [20].

The second research direction, namely LTE-LAA, has been standardized in 3GPP release 13. It was further enhanced in 3GPP release 14 and includes LBT as a core mandate. Recently, techniques to improve the LBT procedure for LTE-LAA have been a very active research topic. LBT provides coexistence by enabling channel sensing and dynamic spectrum access as recommended by 3GPP for unlicensed operation. Initial considerations for LAA examined adopting 802.11's DCF founded on Carrier Sense Multiple Access/Collision Avoidance (CSMA/CA) as basis for LTE-LAA coexistence. However, the drawbacks of not fully exploiting the enhancements of LTE in terms of improved spectral efficiency, low network overhead, and high throughput motivated the consideration of an alternative approach [21,22]. Consequently, solutions ventured to adopt Wi-Fi's DCF and perform suitable optimization to its parameters, mainly focusing on the contention window (CW) size, number of backoff stages, frames per Transmission Opportunity (TxOP), and Arbitration Inter-Frame Spacing (AIFS). Accordingly, several solutions were proposed in literature: [21] Proposed a smaller CW size for LAA nodes that ensures higher spectrum access probability, less spectral access delay and higher throughput. However, results indicated LTE attained an unfair advantage over Wi-Fi whose performance significantly decreased as the number of LTE nodes over the same unlicensed channel increased. In [22], authors defined "graceful coexistence", as the condition in which the performance of an individual node under a network scenario with m Wi-Fi APs and n cellular Base Station (BS)s is not worse than that under a network scenario with only $m + n$ Wi-Fi APs. They solved for an optimal CW size that maximizes the total throughput of the two networks for various data rates and number of nodes. In their solution they utilized a fixed value backoff. In [23] a simplified version of CSMA was pro-

posed where the contention window size was fixed and each time the eNB would choose a random back-off counter uniformly from the same contention window. Moreover, they also proposed a data rate multi-stage back-off scheme, where the eNB would go to a lower data rate stage upon packet collision. Finally, the eNB was allowed to transmit multiple subframes consecutively without the need to sense the channel again. This solution insured higher channel access probability for LAA. However, results also indicated it significantly deteriorated WiFi performance especially as the number of LAA nodes increased. Distinct from previous work, the following solutions assumed LTE stations exchange load configuration information and can infer the accurate number of WiFi stations operating nearby. In [24], an adaptive CW size was proposed where the CW was adjusted based on: 1) the available licensed bandwidth, and 2) the traffic generated by the Wi-Fi network. The CW adjustment was done to maintain a constant collision probability to the Wi-Fi system. [25] Proposed LBT coexistence with TxOP backoff. In this method researchers proposed an adaptive CW and an exponential number of backoff LTE subframes that can be transmitted in a single TxOP. Coexistence is therefore acheived by decreasing the number of subframes transmitted per TxOP as the load of the WLAN increases, in turn lowering LTE's channel occupation. Authors in [26] applied an adaptive exponential CW backoff. The CW adjustment considers channel occupancy, channel condition and cell load by constructing a constrained optimization problem and solving it using a genetic algorithm. Authors in [27] performed a similar analysis with the aforementioned inter-node information exchange, and proposed finding an optimal CW every fixed amount of time that depends on the transmission latency as a quality of service (QoS) indicator, by solving a gradient approaching algorithm they designed. [28] Implemented Wi-Fi DCF with the following changes: 1) Instead of an exponential

backoff, they utilized a linear backoff, and 2) They also set a maximum channel occupancy period for transmission. Few papers were found in literature that proposed a solution aberrant of the DCF. However, some authors examined the interference caused by LTE-LAA as in [29], who proposed adaptive power and bandwidth adjustment to guarantee fair coexistence between a standalone LTE system and WiFi. Authors in [30] proposed a modified Medium Access Control (MAC) protocol for LAA co-existence. In this protocol, a CSMA like LBT technique for LAA in synchronous mode and asynchronous mode was proposed. [31] Exploited frequency reuse between neighboring LAA nodes to reduce interference and allow both systems to coexist. Finally, [32] proposed dynamically switching between traffic offloading and resource sharing schemes, transferring WiFi users to LAA to relinquish some unlicensed resources.

The body of this research work guided the development of the 3GPP study item published in 2015; known as technical report 36.889 [33]. This report was the first official document to specify LTE-LAA's operation and has been the basis of research material assessing LTE-LAA's performance [34–37]. The report defines two operation modes:

1) LBT without random backoff (frame-based LBT) which utilizes a fixed CW window,

2) LBT with a binary exponential CW random backoff (load-based LBT), identical to 802.11's DCF, for coexisting with other incumbents in the unlicensed band.

Nevertheless, the final release 13 3GPP standard specification of TS 36.213 [38] redefined the LBT mechanism adopted in LTE-LAA. Despite it being described to "fundamentally resemble" WiFi's DCF, a specific difference mentioned, alters

the operation of LAA's LBT in comparison to Wi-Fi. This alteration has not been addressed in research work which aims to model the performance of LTE-LAA [15, 36, 39–45]. This shortcoming in literature is indicated in the work found in [46]. However, the authors propose a model that does not conform to the final specification. Transition from every contention window value to the subsequent contention stage is allowed in the their model, contrary to the defined standard. Furthermore, for simplicity, their proposed model only accounts for a specific case of the newly defined K parameter (described fully in the subsequent chapter). Lastly, a collaboration effort between the University of Washington and the University of Chicago found in [47] reports in regards to LTE-LAA: *"Despite significant efforts led by industry, there does not exist as yet a credible analytical model for investigating the coexistence mechanism proposed by 3GPP"*. However, authors note that their analysis does not investigate fair sharing of coexistence which is evident in their use of technology specific data rates in their expressions and analysis work. This deficiency creates an imbalance in actual channel usage time, and results in imprecise interpretation of coexistence fairness. Furthermore, authors assume that Wi-Fi's maximum contention stage occurs for only one additional retransmission which does not conform to the Wi-Fi standard [48]. The paper does not consider inter-network transmission in their expressions for probability of successful transmission, and authors do not investigate homogeneous network coexistence.

In summary, a proper evaluation of Wi-Fi and LTE-LAA LBT coexistence as standardized by 3GPP is still outstanding. The work presented in this dissertation fills this gap. Our work delineates this key fundamental difference between WiFi's DCF and LTE-LAA LBT as described in TS 36.213 of 3GPP rel. 13 and 14. A novel Markov Chain that accurately models the standardized LAA-LBT

is developed and presented. Lastly, by means of the developed model, a comprehensive coexistence performance evaluation of LAA-LBT and 802.11 DCF is carried out, discussed and presented herein.

Chapter 2

LTE in the Unlicensed Band

Worldwide, nation states predominantly consider RF spectrum as a country's exclusive property and one of its national resources, much like land, water, air, oil, gas and minerals. Unlike these, however, RF is a reusable resource. Accordingly, a considerable amount of bandwidth has been globally allocated to provide unlicensed access for short range radio transmissions. These bands, known as the "Unlicensed Spectrum bands", are allocated in different parts of the radio spectrum and are used for a wide variety of applications. The frequency band of current interest for LTE deployment at the time of writing this dissertation is the 5-GHz band. Here there are several hundred MHz of spectrum bandwidth available, although the exact bands available depend upon the country in question. The total of unlicensed spectrum band that is available is comparable to or even more than the amount of the licensed bands used by cellular mobile networks. Figure 2.1 illustrates a bar plot of the available unlicensed bands in the United States (US) region. We observe that the total bandwidth potentially available for use in the 5-GHz Unlicensed National Information Infrastructure (U-NII) radio band is up to 580 MHz .

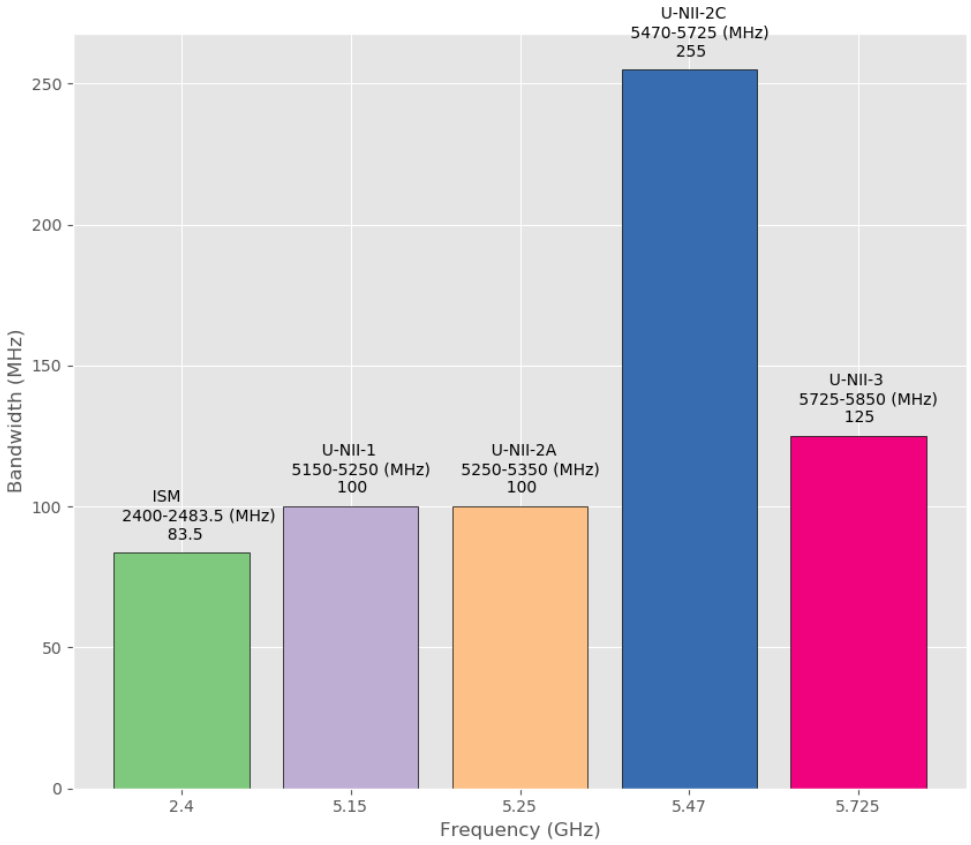

Figure 2.1: Available Unlicensed Spectrum in the USA.

2.1 Unlicensed Spectrum

Because radio signals propagate beyond national borders, governments have long sought to harmonise the allocation of RF bands and their standardization efforts. Globally, the International Telecommunication Union (ITU), part of the United Nations (UN), is the governing body that coordinates the use of both the RF spectrum and space satellites among nation states. This is accomplished through ITU's three Sectors [51]:

1. The Radiocommunication Sector (ITU-R): Responsible for spectrum management principles, techniques, general principles of sharing, spectrum monitoring and long-term strategies for spectrum utilization.

2. The Telecommunication Standardization Sector (ITU-T): develops internationally agreed technical and operating standards.

3. The Telecommunication Development Sector (ITU-D): fosters the expansion of telecommunications infrastructure in developing nations throughout the world.

National service allocations, however, fall within the responsibility of the appropriate national administration. In the U.S, spectrum is managed either by the Federal Communications Commission (FCC) for non-governmental applications, or by the National Telecommunications and Information Administration (NTIA) for governmental applications.

Globally, the two most widely used unlicensed bands are the 2.4-GHz and 5-GHz bands, illustrated in figures 2.2, 2.3 and 2.4. These two bands have their own advantages and disadvantages in various perspectives. The 5-GHz band provides faster data rates at a shorter distance, whereas the 2.4-GHz band offers coverage for greater distances but supports lower rates. Nevertheless, the selection of the 5-GHz band for U-LTE technologies (rather than the 2.4 GHz band) is mainly due to the following reasons:

1. **The Availability of More Channels**: The 2.4-GHz band has 14 defined channels, each 20-MHz wide (In the USA, only 11 of those channels are available, and in Europe only 13). However, those channels excessively overlap with one another. Due to this overlapping, the maximum possible

number of parallel independent connections is limited to 3 channels (channels 1, 6, and 11). In contrast, the 5 GHz band has 21 non-overlapping, 20 MHz channels (or 9 non-overlapping 40 MHz channels). Figure 2.2 illustrates the available 2.4GHz Industrial Scientific and Medical (ISM) Band per region, respectively. Figure 2.3 illustrates the U.S. available 5-GHz ISM Band .

2. **Less Interference Present**: The 2.4-GHz ISM band is increasingly overcrowded, in comparison to the 5-GHz band. This is due to the presence of many existing Wi-Fi devices and consumer products operating numerous wireless radio technologies, including microwave ovens, cordless phones, and wireless body and personal area devices.

3. **Improved Performance**: The 5-GHz band operates on a larger spectrum and does not suffer the aforementioned overcrowding allowing for much better spectrum efficiency and higher data rates.

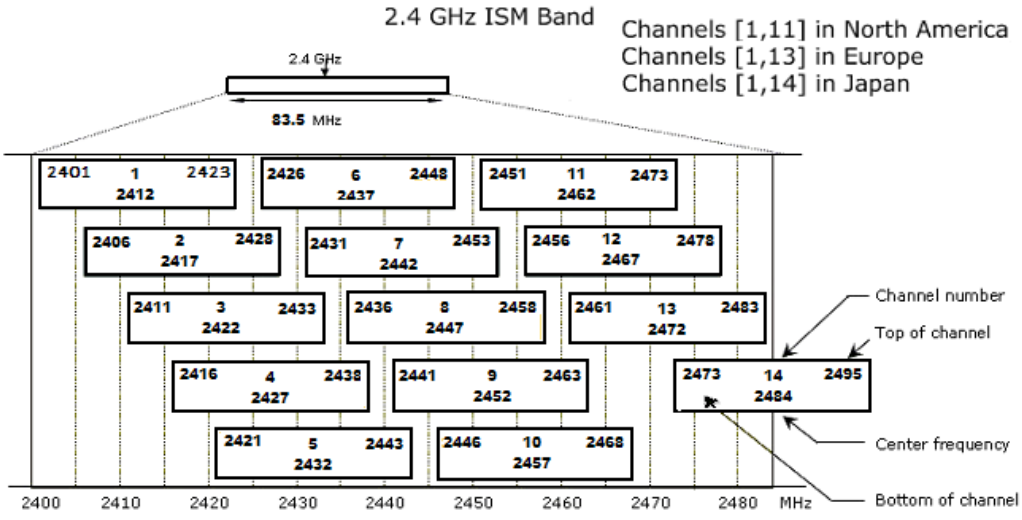

Figure 2.2: The 2.4 GHz ISM Band. [52]

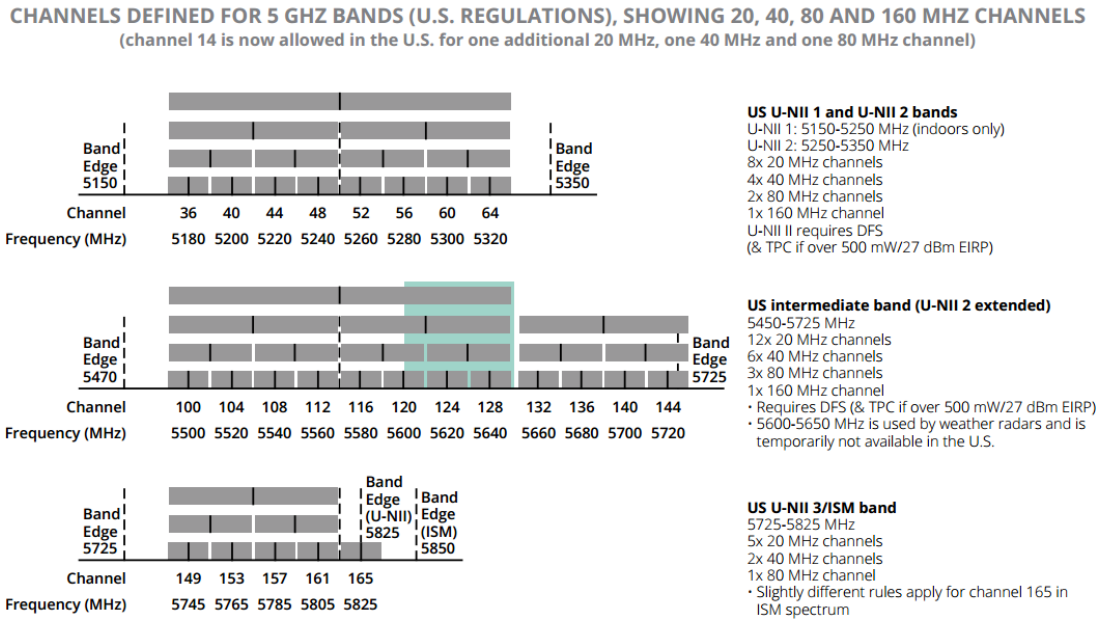

Figure 2.3: The 5-GHz Unlicensed Band. [53]

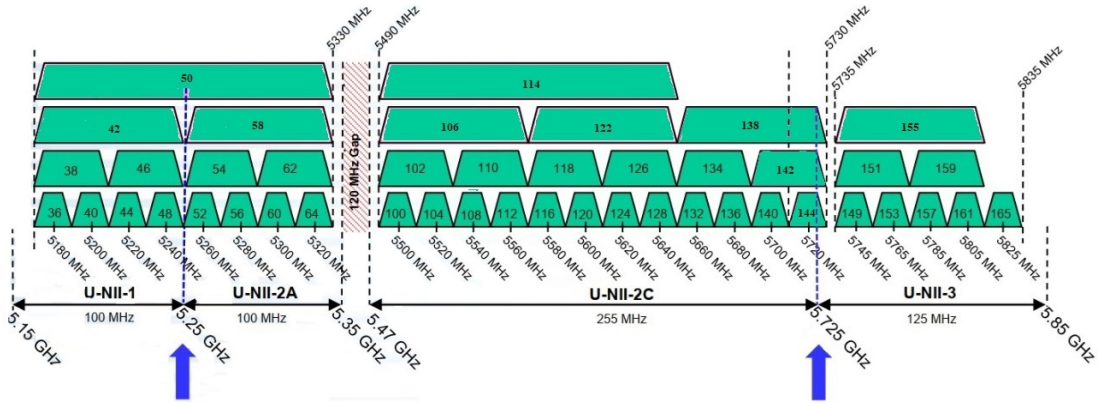

Figure 2.4: The FCC Designated U-NII Bands. [54]

2.2 Regulatory Overview

The Unlicensed National Information Infrastructure is part of the Code of Federal Regulations (CFR), which establishes the FCC's rules for operating the 5-GHz band. In can be found in CFR, Title 47, Part 15 - Radio Frequency Devices,

Subpart E - Unlicensed National Information Infrastructure Devices [55]. In addition to the basic frequency limits, the use of the 5GHz bands for applications carries some regulatory requirements.

1) - **Transmission Power limits**: Limits are set per band i.e. (U-NII 1, U-NII 2, U-NII 2 extended and U-NII 3/ISM). In general, the guidelines restrict client devices to a maximum power limit of 250mW and access points to a limit of 1W. In addition, guidelines are set for antenna directional gain and maximum power spectral density requirements.

2) - **Transmission Power Control (TPC)**: Mandated for U-NII 2 [5.25-5.35 GHz] and U-NII 2 extended [5.47-5.725 GHz] devices for systems with an Equivalent Isotropically Radiated Power (EIRP) of more than 500 mW. The idea of the mechanism is to automatically reduce the used transmission output power when other networks are within range. The power level reduction of a single device should be at least 3 dB (half of the power).

3) - **Dynamic Frequency Selection (DFS)**: Mandated for U-NII 2 [5.25-5.35 GHz] and U-NII 2 extended [5.47-5.725 GHz] devices. Requires the transmitter to continually asses whether the spectrum is used. If such usage is detected the transmitter must vacate the frequency within a specific time (e.g. 10s) and not use it again at least a certain time (e.g. 30 mins) [56]. The purpose is to avoid co-channel operation with radar systems.

4) - **Channel Access Mechanisms**: Finally, in several regions around the world, particularly Japan and Europe, standardization bodies such as the European Telecommunications Standards Institute (ETSI) add additional requirements to avoid channel collisions when two or more than two devices transmit simultaneously in the same channel. These channel access mechanisms are known as

Listen-Before-Talk strategies and are required to be employed. They are broadly divided into 2 types:

1. Frame-Based-Equipment LBT Mechanism (FBE):

   The frame-based LBT transmission structure is not demand driven, but instead it follows a deterministic timeline. Transmissions can only happen at specific times termed the Channel Occupancy Time (CoT), which ranges between a minimum and maximum duration, (e.g. [1- 10] ms). An illustration is depicted in Figure 2.5. As a result, the Clear Channel Assessment (CCA) window also has to be fixed. If the channel is free, then the data is transmitted immediately. If the CCA fails, the transmitter has to relinquish the channel and wait for the next CCA opportunity. Also, an Idle Period (IP) more than 5% of the channel occupancy time is mandatory to leave an oppurnintity for other competitors to access the channel. A flowchart illustrating the process is depicted in figure 2.6.

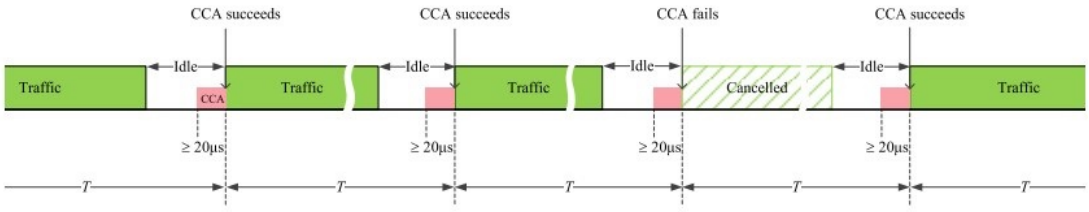

Figure 2.5: Illustration of frame-based LBT, where transmission obeys a fixed time-line with a constant period T. [37]

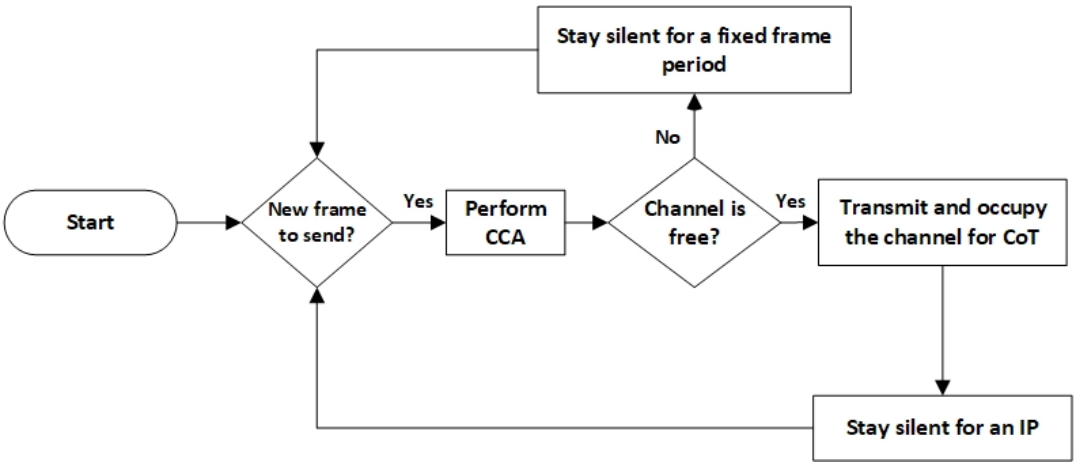

Figure 2.6: Simplified flowchart of FBE LBT mechanism

2. Load-Based-Equipment LBT Mechanism (LBE):

   For load-based transmission as illustrated in Figure 2.7, the transmission time is not fixed. The CCA is performed continuously without abiding by any frame boundaries until it succeeds. At this time, a random back-off (or CCA countdown) timer N is set off to perform an Extended CCA (ECCA) to introduce randomness among competitors for collision avoidance. The random-backoff timer is decremented when a CCA slot succeeds; otherwise, the timer remains frozen. Figure 2.8 illustrates a simplified flow chart of the LBE LBT mechanism.

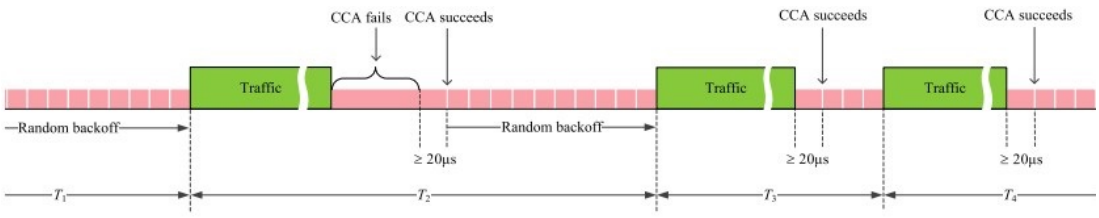

Figure 2.7: Illustration of load-based LBT, where the CCA duration is random, resulting in a variable transmission timeline. [37]

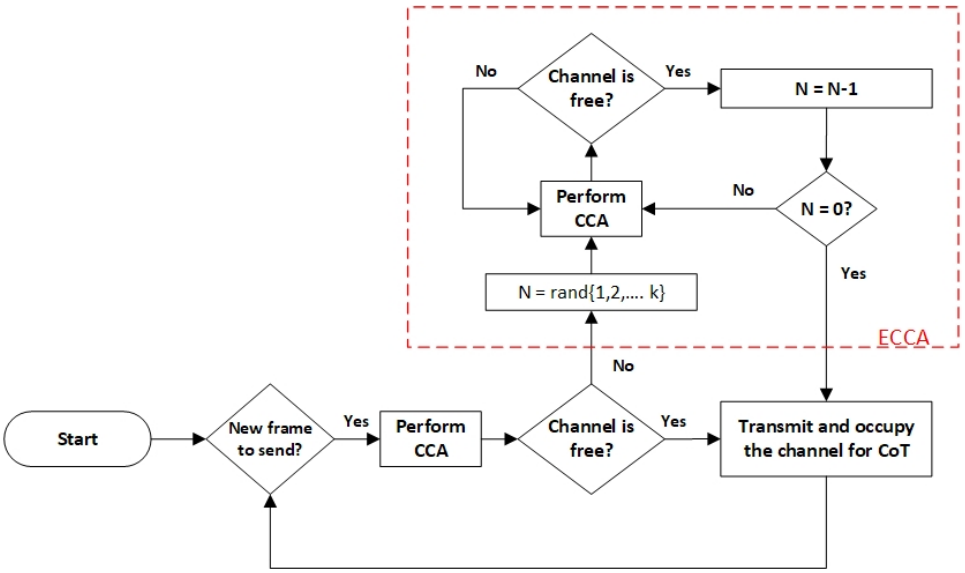

Figure 2.8: Simplified flowchart of LBE

2.3 Wi-Fi

In 1997, the Institute of Electrical and Electronics Engineers (IEEE) introduced the very first version of an ethernet-based Wireless Local Area Network (WLAN) protocol, designated as the 802.11 wireless network standard, and commonly known as Wi-Fi. This first version of the standard provided a low data rate of up to 2 Mbps in the 2.4GHz frequency band and included several media access control (MAC) and physical layer (PHY) technologies that collectively facilitated wireless access and transmission operation. Over the years, many amendments have been introduced to the standard that enhance its capacity and add agility and robustness to the technology. The basic 802.11 MAC layer defined a contention-based channel access mechanism, known as the Distributed Coordination Function (DCF), to exchange data, control and management frames and share the medium between multiple stations operating the unlicensed band. DCF relies on CSMA/CA and an optional 802.11 Request-to-Send (RTS)/ Clear-

to-Send (CTS) messaging scheme for operating and sharing the spectrum. The Point Coordination Function (PCF) is another contention mechanism defined in the initial 1997 802.11 standard, and is available only in "infrastructure" mode. In this mode APs send beacon frames at regular intervals. Between these beacon frames, PCF defines two periods: the Contention Free Period (CFP) and the Contention Period (CP). In the CP, DCF is used. In the CFP, the AP sends Contention-Free-Poll (CF-Poll) packets to each station, one at a time, to give them the right to send a packet. In 2005, IEEE 802.11e-2005 or 802.11e approved an amendment to the IEEE 802.11 standard that defined a new set of quality of service (QoS) enhancements for wireless LAN applications through modifications to the media access control layer. The first QoS design change implemented as part of the 802.11e amendment replaced the one-size-fits all DIFS for all data and management frames, with an Arbitration Inter-Frame Spacing (AIFS), which is dependent on the Access Category (AC) of the frame awaiting transmission. The second major QoS design change implemented as part of the 802.11e amendment was a new coordination function: the hybrid coordination function (HCF). Within the HCF, there are two methods of channel access, similar to those defined in the legacy 802.11 MAC: HCF Controlled Channel Access (HCCA) and Enhanced Distributed Channel Access (EDCA). The HCF (hybrid coordination function) controlled channel access (HCCA) works a lot like PCF. However, in contrast to PCF, in which the interval between two beacon frames is divided into two periods of CFP and CP, the HCCA allows for CFPs being initiated at almost anytime during a CP. The EDCA, however, was defined as an extension to the DCF. It modifies the CCA procedure by setting a different maximum CW size to each QoS class based on the defined traffic AC. The main components of the 802.11's DCF mechanism are the following:

2.3.1 Interframe Spacing (SIFS, PIFS, and DIFS)

There are currently three interframe space (IFS) timers defined in the 802.11 standard as shown in figure 2.9:

- Short interframe space (SIFS)— is the amount of time required for a wireless interface to process a received frame and to respond with a response frame.
- DCF interframe space (DIFS)— is the duration a station must sense the medium to detremine if it is idle or not.
- PCF interframe space (PIFS)— used in the point coordination function, it enables an access point to wait for PIFS duration rather than DIFS to occupy the wireless medium. PIFS duration is less than DIFS and greater than SIFS (DIFS > PIFS > SIFS). Hence an AP operating in the PCF will always have more priority to access the medium.

The interframe spaces (SIFS, PIFS, and DIFS) allow 802.11 to control which traffic gets first access to the channel after carrier sense declares the channel to be free. Generally, 802.11 management frames and frames not expecting contention (a frame that is part of a sequence of frames) use SIFS, and data frames use DIFS.

2.3.2 Random backoff (contention window)

When a data frame using DCF is ready to be sent, it goes through the following steps:

1. The station generates a random backoff number between 0 and a minimum contention window (CWmin).

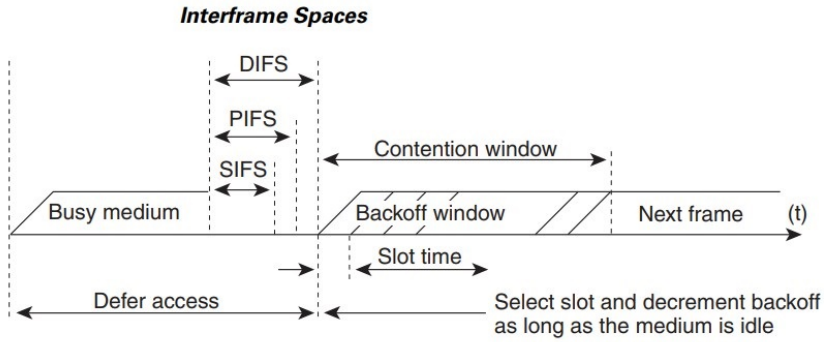

Figure 2.9: Wi-Fi Inter-frame Spaces [58]

2. The station waits until the channel is free for a DIFS interval.

3. If the channel is free, the station begins to decrement the random backoff number, for every slot time that the channel remains free.

4. If the channel becomes busy, such as another station getting to 0 before the current station, the counter decrement stops and Steps 2 through 4 are repeated.

5. If the channel remains free until the random backoff number reaches 0, the frame can be sent

In this mechanism, the process of listening to the channel prior to transmission is the procedure known as Clear Channel Assesment (CCA). The listening period is composed of the DCF DIFS and the random Contention Window (CW) drawn from a maximum CW size that increases exponentially each time a retransmission occurs due to collision. Collision is detected by the absence of an acknowledgment (ACK) frame. The ACK frame is transmitted by the receiving station in SIFS time to indicate correct reception and decoding of the data frame. Figure 2.9 illustrates an example of this procedure for four contending stations in a network.

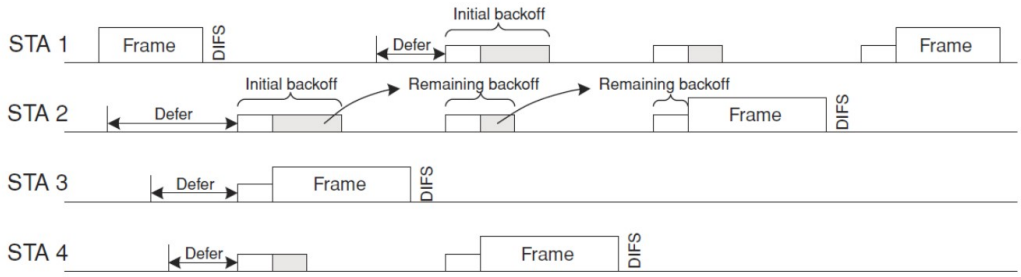

Figure 2.10: Wi-Fi CCA Backoff Procedure Depicting Four Contending Stations [57]

2.3.3 CWmin, CWmax, Retries and Contention Window Scaling

Contention window scaling between CWmin and CWmax occurs as follows in the 802.11 standard:

For the first transmission attempt, the random backoff timer is set to a value between 0 – CWmin. Only when a retransmission is required due to the lack of a returned frame acknowledgement will the possible range grow. For the first and each subsequent retransmission attempt, the contention window will double by a power of 2. This is called binary exponential backoff. Once the window grows to CWmax, it will grow no further. Subsequent retransmission attempts will use the largest contention window range when selecting a random backoff timer value until the frame is either successfully transmitted (and acknowledged) or the maximum number of retransmission attempts is reached (typically somewhere between 8 and 64 attempts. (e.g. Cisco APs default to 64 attempts [58]). Figure 2.11 illustrates this procedure

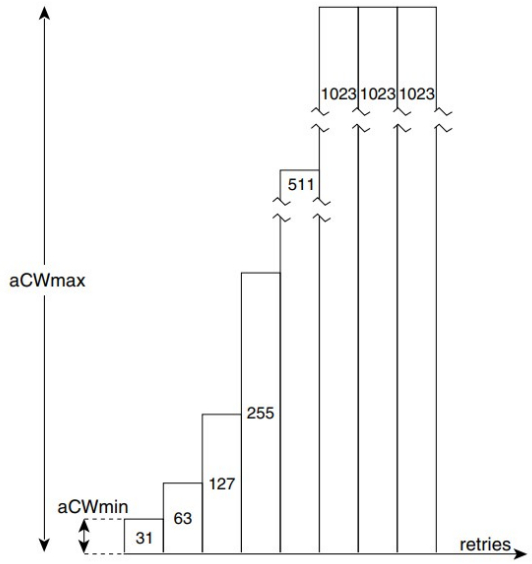

Figure 2.11: Wi-Fi ECCA contention window scaling [58]

2.4 LTE

Considering the regulations imposed on the unlicensed band, existing licensed LTE system techniques employed cannot be directly used for unlicensed band operation. LTE is designed based on the assumption that one operator has exclusive control of a given spectrum. Hence, it will immediately and continuously transmit with a minimum time gap when data traffic is available. Moreover, and in addition to its non-periodical transmissions, LTE also has recurrent transmissions that transfer a variety of control and reference signals. All this makes extending LTE to the unlicensed band by no means a straightforward process. Consequently, different mechanisms have been developed to adapt LTE and make it more pliable to coexist with current incumbents of the unlicensed band. The following presents an overview of these mechanisms and the techniques they have adopted to achieve "fair" coexistence with other unlicensed band technologies.

2.4.1 LTE-U

LTE-U was first introduced by Qualcomm, and later standardized by the LTE-U Forum in 2015 [59]. It is fully compatible with 3GPP Release 10/11, leverages the carrier aggregation technology of 3GPP Release 10 and allows only down-link transmissions in the unlicensed national information infrastructure radio bands (5-GHz band). In order to coexist with current wireless devices operating in this radio band and other LTE-U eNBs, LTE-U employs three separate mechanisms [59–61]:

Dynamic Channel Selection (DCS): DCS enables an LTE-U station to identify and select a "clean" channel for Supplemental Downlink (SDL) transmissions. A clean channel refers to a channel that is not used by any systems in the vicinity of the LTE-U eNB performing the scan. To achieve DCS, channel measurements are performed at the initial power-up and periodically during SDL operation. Interference is measured using the energy detection method which is agnostic to the type and number of interference sources present.

Carrier Sense Adaptive Transmission (CSAT): When no clean channel can be found during the scan process, LTE-U uses a mechanism named Carrier Sense Adaptive Transmission (CSAT) to coexist with current channel incumbents. The CSAT mechanism is based on duty—cycling. In this mechanism, the LTE-U station "profiles" the channel. This means the station monitors the channel utilization and then adaptively adjusts two duration timers; "on-time" and "off-time" durations. During "off-time", the LTE-U eNB ceases all its transmissions. Continuous LTE tranmissions follow during the "on-time" duration. This process repeats periodically with the period ranging from 20—100 msec as

shown in figure 2.12

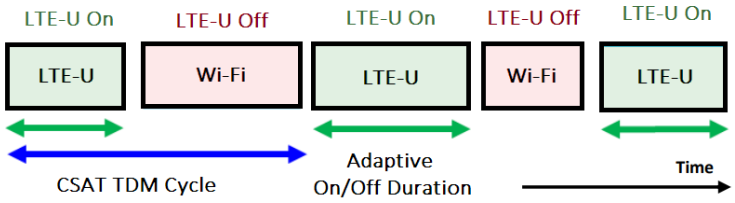

Figure 2.12: LTE-U CSAT operation

Opportunistic Secondary Cell Switch-off: Since the anchor carrier in the licensed band is always available, the SDL carrier in the unlicensed band can be used on an opportunistic basis. This means the SDL carrier is turned off when traffic load is low and can be managed by the licensed carrier alone, or when there is no user within the unlicensed band coverage area. This achieves interference mitigation from continuous Reference Signal (RS) transmissions from LTE-U in the unlicensed channel.

Figure 2.13 depicts the flowchart of LTE-U coexistence operation employing the aforementioned mechanisms. First, 'Channel Selection' enables an LTE-U cell to choose an unoccupied channel. This ensures the interference is avoided between the eNB cell and its neighboring devices and other LTE-U cells, provided an unused channel is available. In the event that no clean channel is available, CSAT is used to apply adaptive Time Division Multiplexing (TDM) transmissions based on long-term carrier sensing, defined to be "around 10's of msec to 200msec and according to the observed medium activities" [61]. Finally, the SDL transmissions can be made opportunistically based on the traffic demand.

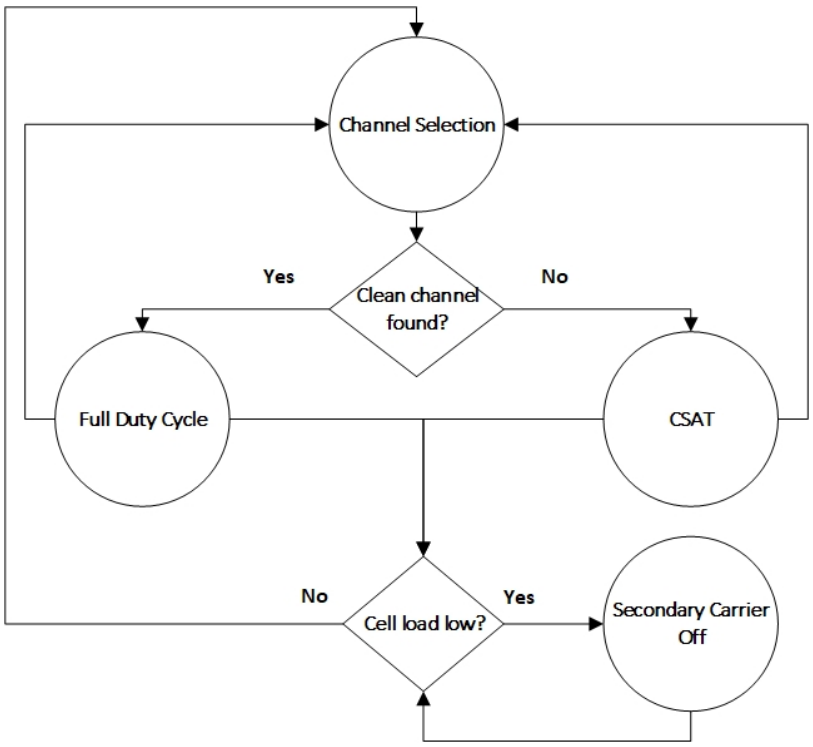

Figure 2.13: LTE-U Co-existence Mechanism Flow Chart [61]

2.4.2 LTE-LAA

LTE-LAA is the second mechanism developed for deploying LTE in the unlicensed band. It was standardized by 3GPP in Release 13, and later enhanced in 3GPP Release 14 (eLAA) to support uplink operation. It is the first standardized mechanism that supports both downlink (DL) and uplink (UL) transmissions and employs LBT as the primary coexistence mechanism. Carrier aggregation with at least one Secondary Cell (SCell) has been specified, with operation limited to the globally available 5-GHz unlicensed spectrum. 3GPP release 13 defines two technical reports (TR 36.889 [33] & TR 36.789 [62]) and six technical specifications (TS 36.300 [63], TS 36.211 [64], TS 36.104 [65], TS 36.141 [66], TS 36.133 [67] & TS 36.213 [38]) that collectively standardize LTE-LAA. A brief description of

each follows: **TS 36.300** [63] gives an overall description of the release Evolved Universal Terrestrial Radio Access (E-UTRA) and Evolved Universal Terrestrial Radio Access Network (E-UTRAN) which define the radio operational aspects of LAA. **TR 36.889** [33] is the initial study item on LAA to the unlicensed spectrum. This report specifies regulatory requirements for the unlicensed band per region, an LAA carrier aggregation feasibility study, deployment scenarios for LAA, design targets and functionalities and finally coexistence evaluations and results. **TR 36.789** [62] specifies the evaluation methodology for multi-node coexistence. This technical report explains how to conduct multi-node tests involving two Rel-13 LAA BSs or one Rel-13 LAA BS and one other wireless system, e.g. IEEE 802.11 system to make sure that the two systems can co-exist in the same unlicensed spectrum. **TS 36.211** [64] Chapter 4, defines a new frame structure type 3 applicable to LAA secondary cell operation with normal cyclic prefix. **TS 36.104** [65] specifies carrier aggregation of component carriers in different operating bands. Chapter 9 presents channel access parameters for LTE-LAA. **TS 36.141** [66] Chapter 9, specifies eNB conformance testing procedures for LBT. Conformance testing is used to verify the accuracy of the energy detection threshold, Maximum Channel Occupancy Time (MCOT) and minimum idle time under normal operating conditions in regards to LAA operation.**TS 36.133** [67] specifies requirements for support of radio resource management for LAA under frame structure 3. **TS 36.213** [38] Chapter 15, defines the channel access procedure and LBT mechanism for LAA.

Release 13 intends LAA to be a global solution framework that achieves effective and fair coexistence with Wi-Fi and adjacent LAA networks deployed by different operators. Accordingly, LTE-LAA technology supports: 1) LBT, 2) Discontinuous transmission on a carrier with limited maximum transmission duration, 3)

Dynamic frequency and carrier selection, 4) Transmit power control and 5) Radio Resource Management (RRM) measurements.

Table 2.1: Mapping Between Channel Access Priority Classes and QCI

Channel Access Priority Class	QCI
1	1, 3, 5, 65, 66, 69, 70
2	2, 7
3	4, 6, 8, 9
4	-

LAA-Listen Before Talk:

LAA applies LBT before transmitting on a SCell. The transmitter senses the channel to determine whether the channel is free or busy. If the channel is determined to be free, transmission may occur. Therefore in LTE-LAA, the configured set of serving cells for a User Equipment (UE) always include at least one SCell operating in the unlicensed spectrum. For downlink LAA, four Channel Access Priority Classes (CAPCs) are defined [38]. The smaller the LBT priority class number, the higher the priority. Table 2.1 depicts which CAPC should be used by traffic belonging to different standardized Qos Class Indicators (QCIs) [68]. LAA mandates that after a successful LBT, if a Downlink (DL) burst within a Physical Downlink Shared Channel (PDSCH) is transmitted, the transmission duration shall not exceed the Maximum Channel Occupancy Time (MCOT) per CAPC denoted $T_{mcot,p}$. The values of $T_{mcot,p}$ are shown in table 2.2 [38].

Table 2.2: Channel Access Priority Class for LTE-LAA DL

Priority Class (p)	m_p	$CW_{min,p}$	$CW_{max,p}$	$T_{mcot,p}$	allowed CW_p sizes
1	1	3	7	2 ms	3,7
2	1	7	15	3 ms	7,15
3	3	15	63	8 or 10 ms	15,31,63
4	7	15	1023	8 or 10 ms	15,31,63,127,255,511,1023

The defer duration T_d, which is the minimum time a node has to wait after the channel becomes idle, is equal to a fixed duration $T_f = 16\mu s$, plus (m_p) consecutive number of time-slot durations $T_{sl} = 9\mu s$ which are identical to WiFi's time-slot. The value of m_p can be found in table 2.2 according to each priority class. Minimum contention window size, $CW_{min,p}$ and maximum contention window size $CW_{max,p}$ per priority class are also shown in table 2.2, where $CW_{min,p} <= CW_p <= CW_{max,p}$. For $p = 3$ and $p = 4$, if the absence of any other technology sharing the carrier can be guaranteed on a long term basis (e.g. by level of regulation), $T_{mcot,p} = 10ms$, otherwise, $T_{mcot,p} = 8ms$.

The LBT mechanism of LTE-LAA is said to fundamentally resemble the CSMA/CA of a 802.11. Before transmitting, the eNB performs Clear Channel Assessment (CCA) using energy detection. The equipment observes the operating channel for the duration of T_d. The operating channel is considered occupied if the energy level in the channel exceeds a threshold X_{Th} during any slots of the duration T_d. If the equipment finds the channel to be clear, and the backoff counter N is equal to zero, it may transmit immediately. If the equipment finds an operating channel occupied, it must not transmit, and instead it must perform an Extended CCA (ECCA) check in which the operating channel is observed for a random duration. Algorithm 1 on page 31 delineates a pseudo-code representing the LTE-LAA LBT mechanism.

Algorithm 1 LAA LBT Mechanism

global variables
    $N = N_{init} \in [0, CW_p]$ random uniform back-off counter.
end global variables
procedure LBT
CCA:
    for $T_d = T_f + (m_p \cdot T_{sl})\mu s$ **do** sense channel
        if Energy detected $< X_{Th}$ **then**
            Check Backoff counter N:
            if $N == 0$ **then**
                Transmit
            else
                goto *ECCA Step 3)*
        else
            goto *ECCA Step 1)*
ECCA:
  Step1):
    Generate $N = N_{init}$
    Go to step 4)
  Step2):
    for $T_d = T_f + (m_p \cdot T_{sl})\mu s$ **do** sense channel
        if Energy detected $< X_{Th}$ **then**
            goto *ECCA Step 3)*
        else
            goto *ECCA Step 2)*
  Step3):
    for $T_{sl} = 9\mu s$ **do** sense channel
        if Energy detected $< X_{Th}$ **then**
            $N = N - 1$
            goto *ECCA Step 4)*
        else
            goto *ECCA Step 2)*
  Step4):
    if $N == 0$ **then**
        Transmit
    else
        goto *ECCA Step 3)*

Contention Window Adjustment:

CW is adjusted based on the Hybrid Automatic Repeat Request (HARQ) Acknowledgment (ACK) feedback. HARQ-ACK feedback can take a value from ACK, Negative Acknowledgment (NACK), and Discontinuous Transmission (DTX). ACK refers to the situation of correct reception, NACK refers to the situation

where control information (i.e., Physical Downlink Control Channel (PDCCH)) is correctly detected but there is an error in the data (i.e., PDSCH) reception, and DTX refers to the situation when a UE misses the control message containing scheduling information (i.e., PDCCH), rather than the data itself (i.e., PDSCH). No HARQ-ACK feedback and DTX are considered as NACK. Furthermore, bundled HARQ-ACK across M subframes are considered as M HARQ-ACK responses. Accordingly, CW_p is adjusted in a similar manner to Wi-Fi DCF. Setting $CW_p = CW_{min,p}$ according to the traffic priority class, when at least four fifths of all HARQ-ACK values corresponding to PDSCH transmission(s) in the reference subframe are NACK then CW_p is increased to the next higher allowed value for that specific priority class according to table 2.2. This corresponds to increasing the backoff stage for retransmissions.

The key difference between Wi-Fi and LAA is found in the contention window adjustment procedure, and occurs when the contention window size W_p reaches the maximum value allowed W_{max}. In Wi-Fi this value is retained as long as collisions continually occur in re-transmissions. Once a certain number of re-transmissions have been attempted (e.g. 16) and if packet collision occurs, the transmitted packet is discarded. In contrast, LAA-LBT specifies a K parameter value in the standard. This value is set by each operator and ranges between 1 and 8. It dictates how many times W_{max} may be used. Once K re-transmissions have been attempted, LAA-LBT resets W_p to W_{min} and re-transmission ensues. Here lies the fundamental difference between both standards.

2.4.3 LWA

LWA, standardized in 3GPP Release 13, is the third mechanism developed for deploying LTE in the unlicensed band. LWA emerged as an unlicensed LTE al-

ternative to LTE-U and LAA systems which require a significant investment in terms of additional hardware (LTE-U/LAA enabled eNBs and UEs) [69]. Furthermore, in contrast to LTE-U and LAA, LWA permits prompt deployment using current technology already commercially available, leveraging the existing LTE and Wi-Fi infrastructures. For LTE data transmissions in the unlicensed band, LWA uses Wi-Fi based medium access and physical layer. This is achieved by splitting the LTE payload at the higher layers into two classes — one transmitted over licensed spectrum bands using the LTE radio, while the other class of traffic is transmitted over unlicensed spectrum using the Wi-Fi radio. As a result, problems arising due to differences in the channel access mechanisms of LTE and WiFi can be alleviated. A conceptual operation architecture of an LWA system is shown in figure 2.14 taken from [70].

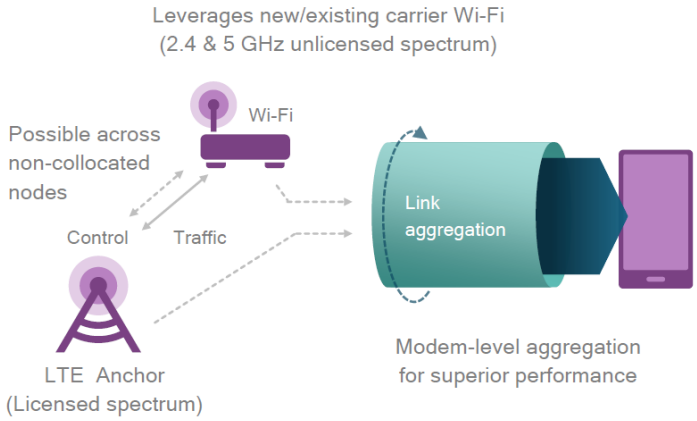

Figure 2.14: LWA Operation Architecture [70]

The LWA eNB performs splitting of the Packet Data Convergence Protocol (PDCP) packets at the PDCP layer, and transmits some of these packets over the LTE air interface, while the remaining are transmitted through the Wi-Fi AP after encapsulating them in Wi-Fi frames. These packets can then be reassembled

at the PDCP layer of the LWA UE.

2.4.4 Multefire

MulteFire is the fourth mechanism developed for deploying LTE in the unlicensed band. Standardized by the MulteFire alliance in specification release 1.0 in December 2016 [71]. It builds upon the enhancements of 3GPP releases 13 and 14. It adopts the LBT procedure of LTE-LAA for coexistence. However, in contrast to all previous mechanisms, it is designed to operate solely in the unlicensed band without the use of a primary anchor in the licensed spectrum [72]. MulteFire is primarily envisioned for entities that have limited or no access to licensed spectrum bands, while giving these entities the benefits of LTE technology. Moreover, MulteFire can also be used by mobile service providers that already have access to licensed spectrum in order to augment their network capabilities. There are two types of architectures defined in the specification [72, 73]:

Neutral Host Network Access Mode: Neutral Host Network (NHN) Access Mode is a self-contained network deployment that provides access to local Internet Protocol (IPR) networks or to the Internet. Mobility is supported between the MulteFire cells within one NHN. The NHN can interact with external service providers to enable services for users (e.g. in restaurants, hotels, venues or public spaces). NHNs can also be deployed as self-contained special purpose private networks in isolated environments (e.g. in private enterprise) providing service to users of enterprise networks. Figure 2.15, taken from [72], illustrates a conceptual schematic of a Multefire cell integration .

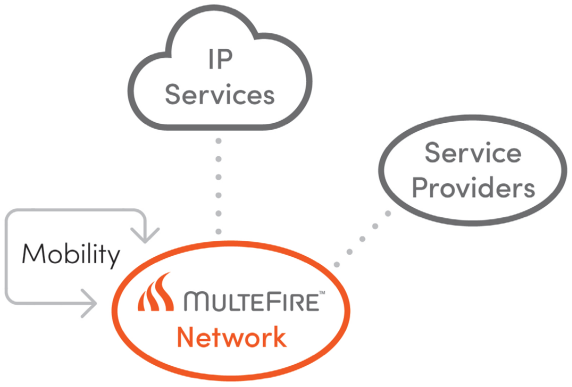

Figure 2.15: Multefire NHN Access Mode

PLMN Access Mode: In the PLMN Access Mode, the MulteFire Radio Access Network (RAN) is connected to a 3GPP Mobile Network Operator (MNO) core as an additional RAN for the PLMN. Figure 2.16 taken from [72] illustrates this. There are two use cases for PLMN access mode:

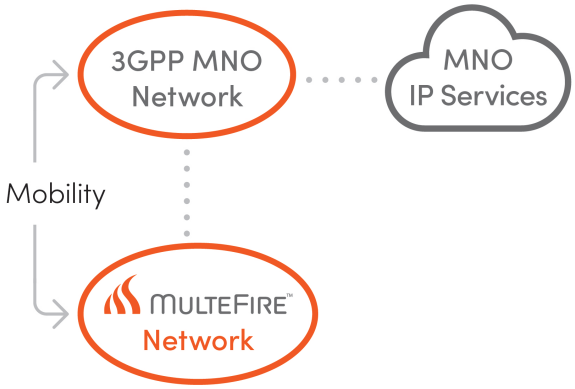

Figure 2.16: Multefire PLMN Access Mode

- MulteFire RAN Connected to an Existing Core Network: In this use case, MulteFire is used as an additional RAN to extend an MNO's network coverage (e.g., where licensed spectrum is not available) or add capacity leveraging existing core network assets.

- MulteFire-only Network: In this use case it is possible for an operator,

without using any licensed band, to deploy an Evolved Packet Core (EPC) with a MulteFire RAN in PLMN Access Mode. Applications envisioned for this use case are special purpose networks (e.g., industrial, mining, offshore) or MNOs without licensed spectrum.

Distinct from LTE-U, LAA, LWA, and as a consequence of the fully unlicensed operation functionality that does not employ a licensed anchor, MulteFire requires support of key procedures such as random access, mobility, and paging in the unlicensed band. However, because of the different nature of transmission on the unlicensed spectrum which is subject to the LBT requirements, some modifications to the legacy LTE system are necessary. These modifications are beyond the scope of this dissertation. However, interested readers are referred to [73] for a detailed explanation of each of the changes.

Chapter 3

Proposed Markov-Chain Model

The LAA LBT mechanism is described to fundamentally resemble the CSMA/CA of Wi-Fi [38]. However, as aformentioned in Chapter 2.2, a key difference is found in the contention window adjustment procedure of LAA-LBT. For WiFi, when the contention window size W_p reaches the maximum value allowed W_{max}, the value is retained as long as collisions continually occur in re-transmissions. Once a maximum number of re-transmissions have been attempted (e.g. 16) the transmitted packet is discarded. In contrast, LAA-LBT specifies a K value. This value is set by each operator and ranges between 1 and 8. It dictates how many times W_{max} may be used. Once K re-transmissions have been attempted, LAA-LBT resets W_p to W_{min} and re-transmission ensues. Here lies the fundamental difference between both standards.

Consistent with previous work in [22, 23, 74] and [75], our analysis and proposed analytical model adopt:

1) A saturated traffic model where all the nodes always have packets to transmit. This permits the problem formulation and analysis work to investigate and highlight the worst-case-scenario of maximum network congestion occurrence and its effect on system performance.

2) An ideal channel where the Bit Error Rate (BER) is 0. This permits the

investigation of the performance bottleneck that occurs due to the underlining coexistence mechanism itself, with the exclusion of external factors, such as channel related data transmission errors that could additionally cause packet loss.

Accordingly, we assume P_l to be the probability of an LAA packet collision occurring. Also, we assume that packet collision is constant and independent and the reference subframe is the starting subframe of the most recent transmission on the carrier made by the eNB, for which at least some HARQ-ACK feedback is expected to be available. Under saturation conditions, the probability that all HARQ-ACK values corresponding to PDSCH transmission(s) in the reference subframe are NACK can be given by $\gamma = P_l$. Let φ be the probability that CW_{max} has occurred K times, then $\varphi = \gamma^{K-1}$. Let i represent the back-off stage, $W_i = 2^i \times W$ for i $\in [0, 1, ...m]$ the contention window. Also let r represent the back-off chosen value. W is the minimum contention window (CW_{min}). We now draw the 2D Markov Chain depicting the operation of LAA-LBT contention window adjustment as shown in figure 3.1. A glossary of variables that are subsequently used in the development and analysis of this model are presented in table 3.1.

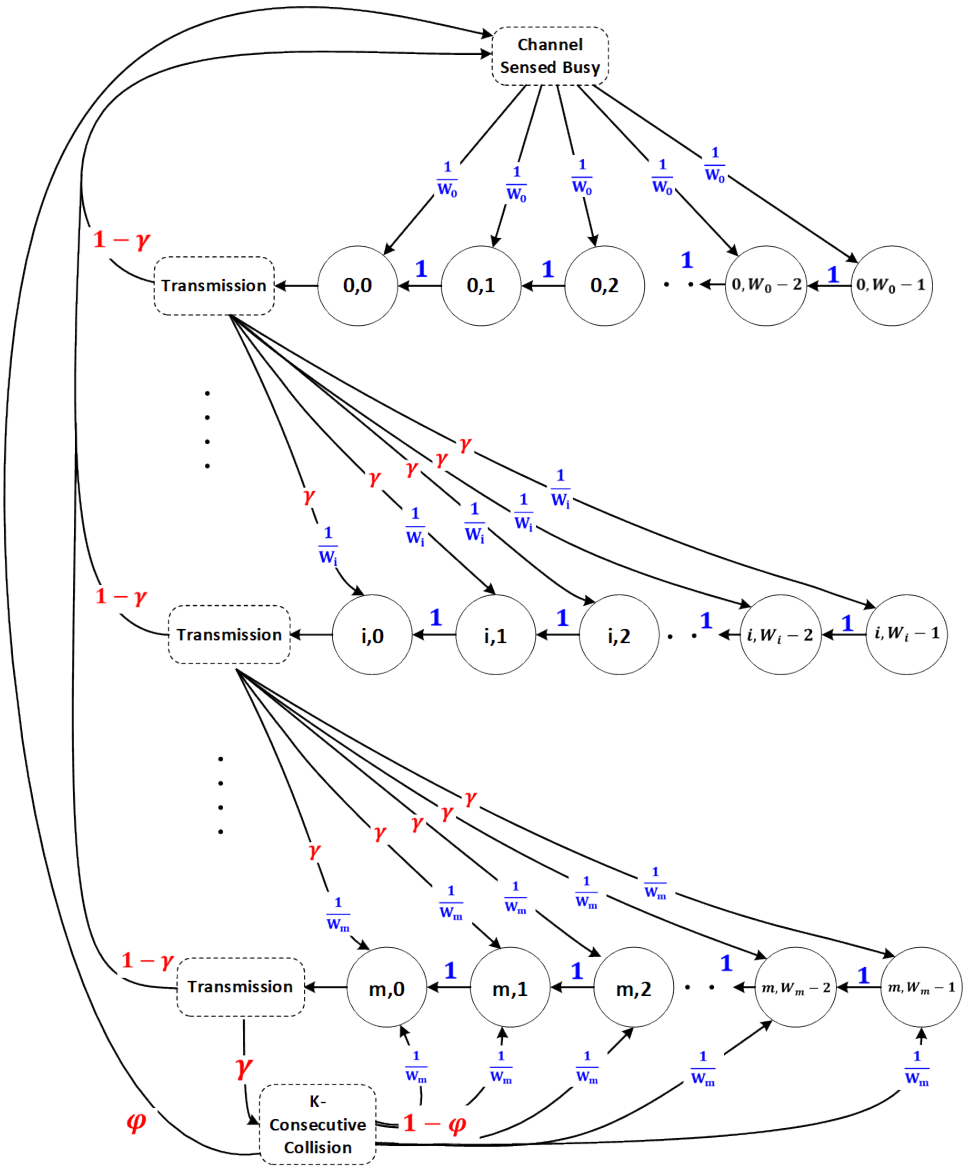

Figure 3.1: Proposed LAA-LBT Markov Chain

Table 3.1: Glossary of Variables Used in Model Development and Analysis

Abbreviation	**Definition**
p	Priority Class ∈ [1,2,3,4]
m_p	Number of backoff stages for priority class p
CW_{min} , W	Minimum contention window size
CW_{max}	Maximum contention window size
$T_{mcot,p}$	Maximum channel occupancy for priority class p
T_d	Transmission differ duration for LAA eNB
T_{sl}	LAA timeslot duration
T_f	Fixed time duration $=16\mu s$
X_{Th}	Energy detection threshold
N	Backoff counter
γ	Probability of LAA transmission burst collision
i	Contention window stage
r	Backoff value chosen
W_i	Contention window size for stage i
$b_{i,r}$	Stationary probability for stage i, backoff value r
m	Maximum backoff stage
τ_l	Probability of transmission for LAA
τ_w	Probability of transmission for Wi-Fi
b_r	Bitrate
γ	Propagation Delay
ACK	Acknowledgment size
$DIFS$	Distributed Interframe Space
$SIFS$	Short Interframe Space
$\sigma = T_{sl}$	Wi-Fi Timeslot duration
P_w	Collision Probability for heterogenous Wi-Fi
P_l	Collision Probability for heterogenous LAA
P_{trw}	Trans. Probability for heterogenous Wi-Fi
P_{trl}	Trans. Probability for heterogenous LAA
P_{sl}	Successful Trans. Probability for heterogenous LAA
P_{sw}	Successful Trans. Probability for heterogenous Wi-Fi
T_{ws}	Time due to successful heterogenous Wi-Fi transmission
T_{ls}	Time due to successful heterogenous LAA transmission
T_{wc}	Time due to collision heterogenous Wi-Fi transmission
T_{lc}	Time due to collision heterogenous LAA transmission
T_a	Time due inter-network transmission

To solve the 2D Markov Chain illustrated in figure 3.1 we begin by deriving the one-step transition probability for each node in the chain. These one-step transition probabilities are subsequently used to derive a stationary probability for each individual node. Finally by imposing the normalizing condition of the Markov Chain and the fact that a transmission at each stage occurs when the counter reaches zero, we derive a closed form solution for the transmission probability of LTE-LAA LBT.

3.1 One-step Transition Probabilities

Calculating the one-step transition probabilities of the Markov Chain of figure 3.1 we find the following expressions:
The probability associated with transitioning from one node on any stage to a consecutive node on that same stage holding a lower back-off value, occurs when the channel is sensed to be idle and the counter is decremented, and is expressed as:

$$p(i, r|i, r+1) = 1 \qquad : i \in [0, m],\ r \in [0, W_i - 2],$$

The probability associated with transitioning from the 0^{th} node on any stage, excluding the last stage, to a node on the first stage, is the probability that no collision takes place following a transmission, and is expressed as:

$$p(0, r|i, 0) = \frac{(1-\gamma)}{W_0} \qquad : i \in [0, m-1],\ r \in [0, W_i - 1],$$

The probability associated with transitioning from the 0^{th} node on any stage to a node on the one-step consecutive higher order stage, occurs when a collision takes place following a transmission, and is expressed as:

$$p(i, r|i-1, 0) = \frac{\gamma}{W_i} \quad : i \in [1, m],\ r \in [0, W_i - 1],$$

For the last stage in the Markov chain we find the following two expressions: The probability associated with transitioning from the 0^{th} node on the last stage back to a node on the last stage again, occurs when retransmission takes place following a collision on the last stage, and, the set K parameter value has not been realized. This is expressed as:

$$p(m, r|m, 0) = \frac{\gamma - \gamma^K}{W_m} \quad : r \in [0, W_m - 1],$$

Finally, the probability associated with transitioning from the 0^{th} node on the last stage to a node on the first stage, is the probability that no collision takes place after transmission, or, a collision does in fact occur, but the set K parameter value has been realized. This probability is expressed as:

$$p(0, r|m, 0) = \frac{\gamma^K - \gamma + 1}{W_0} \quad : r \in [0, W_0 - 1].$$

3.2 Stationary Probabilities

Using the one-step transition probabilities obtained above, we proceed to derive the stationary probability for each node in the chain. For this, let $b_{i,r}$ represent the stationary probability of node r on stage i, and t represent time. We express the stationary probability as $b_{i,r} = lim_{t\to\infty} p\{i, r\}$. We find the following expressions:

Case of $i = 0$ and $r \in [1, W_0 - 1]$:

The stationary probability of a node on the first stage when $i = 0$ and $r \in [1, W_0 - 1]$ is equal to the stationary probability of its consecutive node on the first stage holding a higher back-off value, plus the sum of the stationary probabilities of the 0^{th} node of all stages except the last one when a successful transmission occurs, plus the stationary probability of the 0^{th} node on the last stage when a successful transmission occurs, or a collision happens when the set K parameter value has been realized. Where each stationary probability is multiplied by its one-step transition probability. Therefore, for $i = 0$:

$$b_{i,r} = b_{i,r+1} \cdot 1 + \sum_{j=0}^{m-1} \frac{b_{j,0} \cdot (1-\gamma)}{W_i} + b_{m,0} \cdot \frac{(\gamma^K - \gamma + 1)}{W_i},$$

$$b_{i,r+1} = b_{i,r+2} \cdot 1 + \sum_{j=0}^{m-1} \frac{b_{j,0} \cdot (1-\gamma)}{W_i} + b_{m,0} \cdot \frac{(\gamma^K - \gamma + 1)}{W_i},$$

$$\ddots$$

$$b_{i,W_i-1} = \sum_{j=0}^{m-1} \frac{b_{j,0} \cdot (1-\gamma)}{W_i} + b_{m,0} \cdot \frac{(\gamma^K - \gamma + 1)}{W_i}.$$

accordingly, by substituting and summing these expressions we find for $i = 0$ and $r \in [1, W_0 - 1]$ the stationary probability is expressed as:

$$b_{i,r} = \frac{W_i - r}{W_i} \cdot \left(\sum_{j=0}^{m-1} b_{j,0} \cdot (1 - \gamma) + b_{m,0} \cdot (\gamma^K - \gamma + 1) \right). \tag{3.1}$$

Case of $i \in [1, m - 1]$ and $r \in [1, W_i - 1]$:

For the nodes where $i \in [1, m - 1]$ and $r \in [1, W_i - 1]$ we find the stationary probability is equal to the stationary probability of the consecutive node on the same stage holding a higher back-off value, plus the stationary probability of the

0^{th} node of the previous lower order stage. Where each stationary probability is multiplied by its one-step transition probability. Therefore, for $i \in [1, m-1]$:

$$b_{i,r} = b_{i,r+1} \cdot 1 + b_{i-1,0} \cdot \frac{\gamma}{W_i},$$

$$b_{i,r+1} = b_{i,r+2} \cdot 1 + b_{i-1,0} \cdot \frac{\gamma}{W_i},$$
$$\ddots$$
$$b_{i,W_i-1} = b_{i-1,0} \cdot \frac{\gamma}{W_i}.$$

accordingly, by substituting and summing these expressions we find for $i \in [1, m-1]$ and $r \in [1, W_i - 1]$ the stationary probability is expressed as:

$$b_{i,r} = \frac{W_i - r}{W_i} \cdot b_{i-1,0} \cdot \gamma. \tag{3.2}$$

Case of $i = m$ and $r \in [1, W_m - 1]$:

For $i = m$ and $r \in [1, W_m - 1]$ we find the stationary probability of a node is equal to the stationary probability of the consecutive node on the same stage holding a higher back-off value, plus the stationary probability of the 0^{th} node of the previous lower order stage, plus the stationary probability of the 0^{th} node of the last stage when retransmission takes place following a collision on the last stage and the set K parameter value has not been realized. Where each stationary probability is multiplied by its one-step transition probability. Thus, for $i = m$:

$$b_{i,r} = b_{i,r+1} \cdot 1 + b_{i-1,0} \cdot \frac{\gamma}{W_i} + b_{i,0} \cdot \frac{(\gamma - \gamma^K)}{W_i},$$

$$b_{i,r+1} = b_{i,r+2} \cdot 1 + b_{i-1,0} \cdot \frac{\gamma}{W_i} + b_{i,0} \cdot \frac{(\gamma - \gamma^K)}{W_i},$$
$$\ddots$$
$$b_{i,W_i-1} = b_{i-1,0} \cdot \frac{\gamma}{W_i} + b_{i,0} \cdot \frac{(\gamma - \gamma^K)}{W_i}.$$

Therefore, by substituting and summing these expressions for $i = m$ and $r \in [1, W_m - 1]$ we find the stationary probability is expressed as:

$$b_{i,r} = \frac{W_i - r}{W_i} \cdot \Bigg(b_{i-1,0} \cdot \gamma + b_{i,0} \cdot (\gamma - \gamma^K) \Bigg). \tag{3.3}$$

Equations (3.1), (3.2) and (3.3) are summarized for $r \in [1, W_i - 1]$ as:

$$b_{i,r} = \\ \frac{W_i - r}{W_i} \cdot \left\{ \begin{array}{cc} \sum_{j=0}^{m-1} b_{j,0} \cdot (1-\gamma) + b_{m,0} \cdot (\gamma^K - \gamma + 1) & : \ i = 0 \\ b_{i-1,0} \cdot \gamma & : \ 0 < i < m \\ b_{i-1,0} \cdot \gamma + b_{i,0} \cdot (\gamma - \gamma^K) & : \ i = m \end{array} \right\} \tag{3.4}$$

We now find expressions for each of the factors $b_{i,0}$, $b_{i-1,0}$, $b_{m,0}$, $b_{m-1,0}$, and $\sum_{j=0}^{m-1} b_{j,0}$ as follows:

Case of $r = 0$ and $0 < i < m$:

We find the stationary probability $b_{i,r}$ is equal to the stationary probability of the subsequent node on the same stage with a higher back-off value plus the 0^{th} node of the previous lower order stage, each multiplied by their one-step transition probability. As such:

$$\begin{aligned} b_{i,0} &= b_{i,1} \cdot 1 + b_{i-1,0} \cdot \tfrac{\gamma}{W_i}, \\ b_{i,1} &= b_{i,2} \cdot 1 + b_{i-1,0} \cdot \tfrac{\gamma}{W_i}, \\ b_{i,2} &= b_{i,3} \cdot 1 + b_{i-1,0} \cdot \tfrac{\gamma}{W_i}, \\ &\ddots \\ b_{i,W_i-1} &= b_{i-1,0} \cdot \tfrac{\gamma}{W_i}. \end{aligned}$$

By substituting and summing these expressions we express:

$$b_{i,0} = b_{i-1,0} \cdot \gamma$$

Also,

$$b_{m-1,0} = b_{m-2,0} \cdot \gamma,$$
$$b_{m-2,0} = b_{m-3,0} \cdot \gamma,$$
$$\ddots$$
$$b_{1,0} = b_{0,0} \cdot \gamma$$

Summing this expression leads to:

$$b_{m-1,0} = \gamma^{m-1} \cdot b_{0,0},$$

and therefore:

$$b_{i,0} = \gamma^i \cdot b_{00} \tag{3.5}$$

Case of $r = 0$ and $i = m$:

$$b_{m,0} = b_{m,1} \cdot 1 + b_{m-1,0} \cdot \tfrac{\gamma}{W_m} + b_{m,0} \cdot \tfrac{(\gamma - \gamma^K)}{W_m},$$
$$b_{m,1} = b_{m,2} \cdot 1 + b_{m-1,0} \cdot \tfrac{\gamma}{W_m} + b_{m,0} \cdot \tfrac{(\gamma - \gamma^K)}{W_m},$$
$$\ddots$$
$$b_{m,W_m-1} = b_{m-1,0} \cdot \tfrac{\gamma}{W_m} + b_{m,0} \cdot \tfrac{(\gamma - \gamma^K)}{W_m}$$

This leads to:

$$b_{m,0} = b_{m-1,0} \cdot \gamma + b_{m,0} \cdot (\gamma - \gamma^K)$$

$$b_{m,0} \cdot (1 - \gamma + \gamma^K) = b_{m-1,0} \cdot \gamma$$

Using equation (3.4) we find the stationary probability to be:

$$b_{m,0} = \frac{\gamma^m}{\gamma^K - \gamma + 1} \cdot b_{0,0}. \tag{3.6}$$

We now find $\sum_{j=0}^{m-1} b_{j,0}$ as follows:

$$\sum_{j=0}^{m-1} b_{j,0} = b_{0,0} + b_{1,0} + b_{2,0} + ... + b_{m-1,0},$$

$$= b_{0,0} + \gamma \cdot b_{0,0} + \gamma^2 \cdot b_{0,0} + ... + \gamma^{m-1} \cdot b_{0,0},$$

$$= b_{0,0}\Big(1 + \gamma + \gamma^2 + ... + \gamma^{m-1}\Big)$$

Using the geometric series of:

$$\sum_{x=0}^{n-1} a.y^x = a \cdot \frac{1-y^n}{1-y}.$$

We find the sum factor of equation (3.1) to be,

$$\sum_{j=0}^{m-1} b_{j,0} = b_{0,0} \cdot \frac{1-\gamma^m}{1-\gamma}. \tag{3.7}$$

We now use equations (3.5), (3.6) and (3.7) to summarize and express (3.4)'s formula as:

For i = 0:

$$b_{i,r} = \tfrac{W_i - r}{W_i} \cdot \left((1-\gamma) \cdot \textstyle\sum_{j=0}^{m-1} b_{j,0} + b_{m,0} \cdot (\gamma^K - \gamma + 1) \right)$$

$$= \tfrac{W_i - r}{W_i} \cdot \left((1-\gamma) \cdot \left(\tfrac{1-\gamma^m}{1-\gamma} \cdot b_{0,0} \right) + \left(\tfrac{\gamma^m}{\gamma^K - \gamma + 1} \cdot b_{0,0} \right) \cdot (\gamma^K - \gamma + 1) \right)$$

$$= \tfrac{W_i - r}{W_i} \cdot b_{0,0}.$$

For $0 < i < m$:

$$b_{i,r} = \tfrac{W_i - r}{W_i} \cdot \Big(b_{i-1,0} \cdot \gamma \Big),$$

$$= \frac{W_i - r}{W_i} \cdot \Big(\gamma^{i-1} \cdot b_{0,0} \cdot \gamma \Big),$$

$$= \frac{W_i - r}{W_i} \cdot \Big(\gamma^{i} \cdot b_{0,0} \Big),$$

$$= \frac{W_i - r}{W_i} \cdot b_{i,0} \quad .$$

Finally, for $i = m$:

$$b_{i,r} = \frac{W_i - r}{W_i} \cdot \Big(b_{i-1,0} \cdot \gamma + b_{i,0} \cdot (\gamma - \gamma^K) \Big),$$

$$= \frac{W_i - r}{W_i} \cdot \Big(\gamma^{m-1} \cdot \gamma \cdot b_{0,0} + b_{m,0} \cdot (\gamma - \gamma^K) \Big),$$

$$= \frac{W_i - r}{W_i} \cdot \Big(\gamma^{m} \cdot b_{0,0} + \frac{\gamma^m}{\gamma^K - \gamma + 1} \cdot (\gamma - \gamma^K) \cdot b_{0,0} \Big),$$

which simplifies to:

$$= \frac{W_i - r}{W_i} \cdot \Big(\frac{\gamma^m}{\gamma^K - \gamma + 1} \cdot b_{0,0} \Big),$$

$$= \frac{W_i - r}{W_i} \cdot b_{m,0}$$

Therefore, we can now express $b_{i,r}$ as:

$$b_{i,r} = \frac{W_i - r}{W_i} \cdot b_{i,0} \tag{3.8}$$

Where, $i \in [0, m]$, and $r \in [0, W_i - 1]$.

We now solve the expression in (3.8), and thus the Markov chain expressed as a function of $b_{0,0}$, by imposing the normalizing condition:

$$1 = \sum_{i=0}^{m} \sum_{r=0}^{W_i - 1} b_{i,r}$$

$$= \sum_{i=0}^{m} \sum_{r=0}^{W_i - 1} \frac{W_i - r}{W_i} \cdot b_{i,0}$$

$$= \sum_{i=0}^{m} b_{i,0} \cdot \left(\frac{W_i + 1}{2} \right)$$

$$= \frac{1}{2} \sum_{i=0}^{m} (b_{i,0} \cdot W_i + b_{i,0})$$

$$= \frac{1}{2} \left[\sum_{i=0}^{m} b_{i,0} \cdot 2^i W + \sum_{i=0}^{m} b_{i,0} \right]$$

$$= \frac{1}{2} \left[\sum_{i=0}^{m-1} (b_{i,0} \cdot 2^i W) + b_{m,0} \cdot 2^m W + \sum_{i=0}^{m-1} b_{i,0} + b_{m,0} \right]$$

$$= \frac{b_{0,0}}{2} \left[\sum_{i=0}^{m-1} (2\gamma)^i \cdot W + \frac{(2\gamma)^m}{\gamma^K - \gamma + 1} \cdot W + \frac{1 - \gamma^m}{1 - \gamma} + \frac{\gamma^m}{\gamma^K - \gamma + 1} \right]$$

$$= \frac{b_{0,0}}{2} \cdot \left[\frac{(1-\gamma)(1 + W \cdot (2\gamma)^m) + \gamma^K (1 - \gamma^m)}{(1-\gamma)(\gamma^K - \gamma + 1)} + \frac{W(1 - (2\gamma)^m)}{1 - (2\gamma)} \right] \tag{3.9}$$

We find $b_{0,0}$ by solving the expression:

$$b_{0,0} = \frac{2 \cdot (1-\gamma)(\gamma^K - \gamma + 1)(1 - (2\gamma))}{(1-\gamma)(1-2\gamma)(1 + W(2\gamma)^m) + \gamma^K (1 - \gamma^m)(1 - 2\gamma) + W(1 - (2\gamma)^m)(1-\gamma)(\gamma^K - \gamma + 1)} \tag{3.10}$$

We can now express the probability of an LTE-LAA node transmitting, denoted as τ_L, as:

$$\tau_L = \sum_{i=0}^{m} b_{i,0} = \sum_{i=0}^{m-1} b_{i,0} + b_{m,0}$$

$$= b_{0,0} \cdot \left(\frac{1-\gamma^m}{1-\gamma} \right) + \left(\frac{\gamma^m}{\gamma^K - \gamma + 1} \right) \cdot b_{0,0}$$

$$= b_{0,0} \cdot \left(\frac{\gamma^K - \gamma + 1 - \gamma^{m+K}}{(1-\gamma) \cdot (\gamma^K - \gamma + 1)} \right) \tag{3.11}$$

Using (3.10) in (3.11) and solving we find:

$$\tau_L = \frac{A}{B + C + D} \tag{3.12}$$

where:

$$A = 2 \cdot (1 - 2\gamma) \cdot (\gamma^K - \gamma + 1 - \gamma^{m+K})$$

$$B = (1 - \gamma) \cdot (1 - 2\gamma) \cdot (1 + W(2\gamma)^m)$$

$$C = \gamma^K \cdot (1 - \gamma^m) \cdot (1 - 2\gamma)$$

$$D = W \cdot (1 - (2\gamma)^m) \cdot (1 - \gamma) \cdot (\gamma^K - \gamma + 1)$$

Recalling W refers to the minimum contention window size allowed; W_{min}.
It is noted that when $m = 0$, i.e. (No exponential backoff is considered), the probability of transmission in (3.12) simplifies to: $\tau_L = \frac{2}{W+1}$ matching the probability of transmission for 802.11 as found in [74].

Table 3.2: Station Channel Access Parameters

Parameter	Unit
Priority Class	P = 4
m_p	7
CW_p: Allowed sizes	[15,31,63,127,255,511,1023]
$T_{mcot,p}$: Maximum channel occupancy time	8ms
E[P]: Packet Payload	8184 bits
br: bitrate	1Mbps
δ: Propagation Delay	$1\mu s$
H: Packet Header (PHY + MAC)	400bits
ACK: HARQ-ACK	240bits
σ: TimeSlot	$9\mu s$
DIFS: $16\mu s + (m_p + \sigma)$	$79\mu s$
SIFS	$16\mu s$

3.3 Model Validation

To validate the accuracy of the proposed model, numerical results obtained from the developed analytical model are compared with those obtained from simulation using an LTE-LAA LBT simulator. The simulator emulates the standardized LBT mechanism and is subjected to the constraints assumed in this work with regards to the normalized saturation throughput. Subsequently, we examine how the medium access mechanism and the contention window size adjustment, occupancy time and number of stations affect throughput performance of the system.

For this, we consider a network of n neighboring stations utilizing the LTE-LAA LBT mechanism. The probability γ, that any single transmission of a BS encounters a collision, is the probability that in a time slot, at least one of the n-1 remaining stations transmits. i.e.

$$\gamma = 1 - (1 - \tau_L)^{n-1} \tag{3.13}$$

Solving the non-linear system of equations found in (3.12) and (3.13) using numerical techniques yields the probability of collision, and the probability of transmission, γ and τ_L, respectively. We define the normalized system throughput S, as the fraction of time the channel is used to successfully transmit payload bits. This is expressed as:

$$S = \frac{P_s P_{tr} EP}{(1 - P_{tr})\sigma + P_{tr} P_s T_s + P_{tr}(1 - P_s) T_c} \tag{3.14}$$

Where $P_{tr} = 1-(1-\tau_L)^n$ is the probability of at least one transmission occurring in the considered time slot, $P_s = \frac{n\tau_L(1-\tau_L)^{n-1}}{P_{tr}}$ is the probability of a successful transmission, σ is the time slot duration. $EP = T_{mcot,p}$. T_s and T_c were fixed for both numerical and simulation analysis at 8.9ms and 8.7ms respectively according to LAA channel access priority class $P = 4$.

Numerical results were computed using Matlab by solving equations (3.12) and (3.13) with the parameters of Table 3.2. Simulation of LAA-LBT procedure was done in a LTE-LAA LBT simulator built in Python that ran for n contending stations for 10^8 time steps utilizing the same parameters. The simulation starts with all n nodes attempting to transmit and consequently backing off according to the standardized LAA LBT mechanism, described fully in pseudo code of algorithm 1 on page 31 of chapter 2. In this, each node maintains a backoff value, backoff stage, and a re-transmission counter that are updated upon successful transmission or collision. Transmission, collision, and idle times are tracked to estimate S as an average of x simulation runs. This was repeated for maximum back-off stages $m = [2, 4, 6]$ and LAA-LBT parameter $K = 1$.

3.3.1 Validation Results:

The outcome of the validation examination can be seen in Figure 3.2. The figure depicts a comparison plot between both numerical and simulated saturation throughput results as recorded by the LTE-LAA LBT simulator and the Markov Chain numerical model output. The Root Mean Squared Error (RMSE) calculated between the two plots was equal to 0.0045. This signifies high model accuracy, and as a result, it can be concluded that the developed Markov Chain accurately models the 3GPP LTE-LAA LBT mechanism defined in TS 36.213.

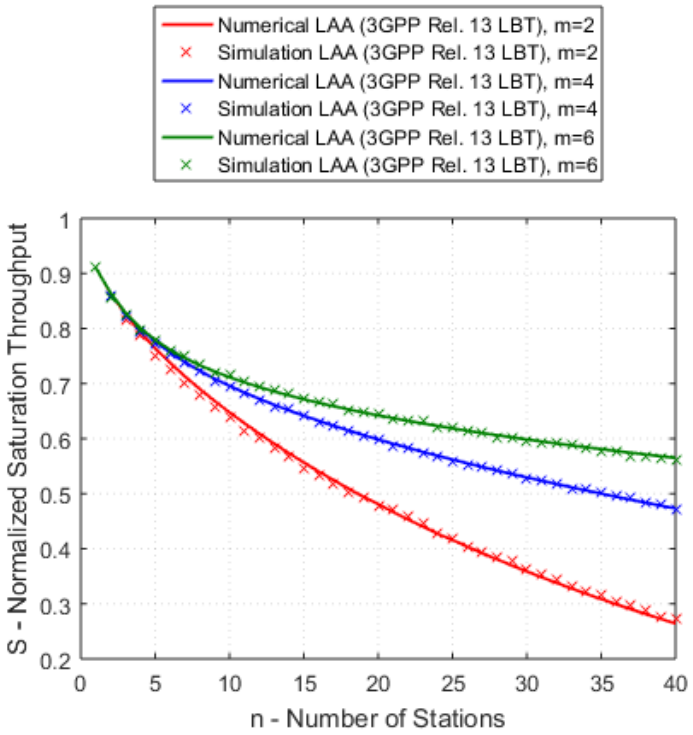

Figure 3.2: Numerical vs. Simulation Validation Results

3.4 LTE-LAA LBT Performance Analysis

In this section LTE-LAA LBT performance analysis is developed and demonstrated contrasting the standardized 3GPP LTE-LAA LBT τ_L, using the numerical model developed, and Wi-Fi's LBT mechanism with a transmission probability τ_w given by [74] as:

$$\tau_w = \frac{2(1-2P_w)}{(1-2P_w)(W+1)+p_wW(1-(2p_w)^m)}. \tag{3.15}$$

The objective of the analysis in this section is to examine and delineate the performance difference between the LBT mechanisms of LAA and Wi-Fi distinctly. This serves to attain a clear understanding of what effect the newly defined K parameter has on the performance of LTE-LAA LBT. To achieve this, we consider two isolated networks each composed of n neighboring stations utilizing the LTE-LAA LBT mechanism and the Wi-Fi LBT mechanism, respectively. We adopt the normalized saturation throughput expression defined in (3.14) as our metric for performance measurement, and we set $T_c = (H+EP)/b_r + DIFS + \delta$ and $T_s = (H+EP)/b_r + SIFS + \delta + ACK + DIFS + \delta$, as calculated from table 3.2, for both networks.

3.4.1 Performance Analysis Results:

We regard in figure 3.3 the normalized saturation throughput of LTE-LAA for values of $K \in [1, 2, 4, 6, 7, 16]$ and $n \in [2, 40]$ nodes. We observe as the number of n co-channel LAA stations operating LAA-LBT increases, the saturation throughput drops below than that of n co-channel Wi-Fi APs operating Wi-Fi's

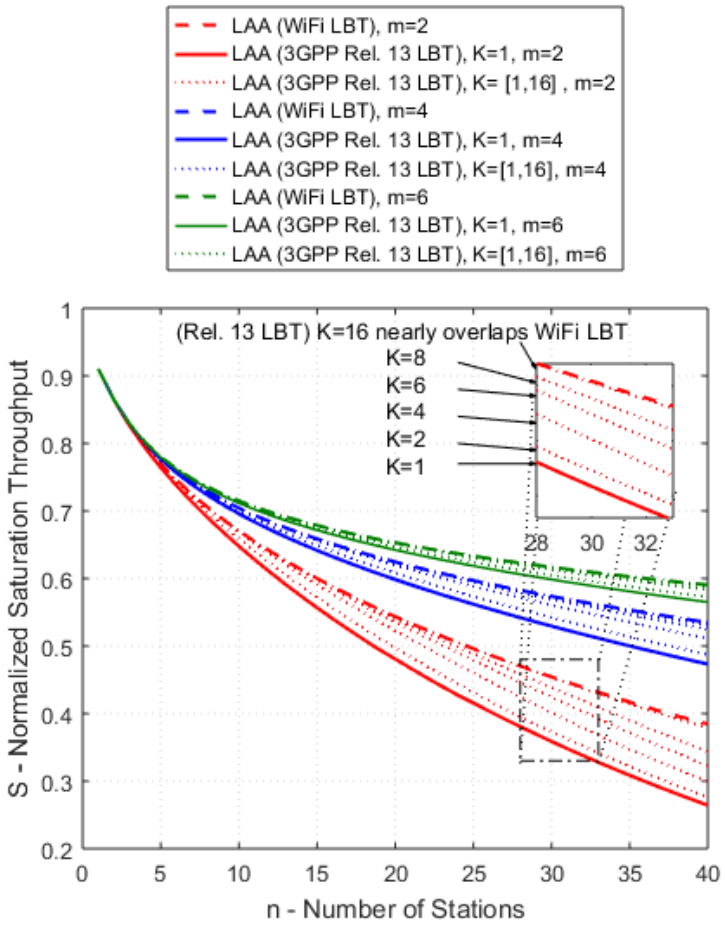

Figure 3.3: Normalized Saturation Throughput for $K \in [1, 2, 4, 6, 8, 16]$

LBT. This is confirmed in figure 3.4 where we can observe that LTE-LAA LBT achieves a higher probability of transmission with an increasing number of contending nodes. This result is clarified in the following analysis.

K-Parameter Analysis:

As the number of nodes in the network increases, collision will increase as well, resulting in higher backoff stages to be selected for both LAA and Wi-Fi. However, in saturation, and as LAA-LBT resets CW_p once the maximum backoff stage retransmission has been reached K times, the lower stage will increase transmis-

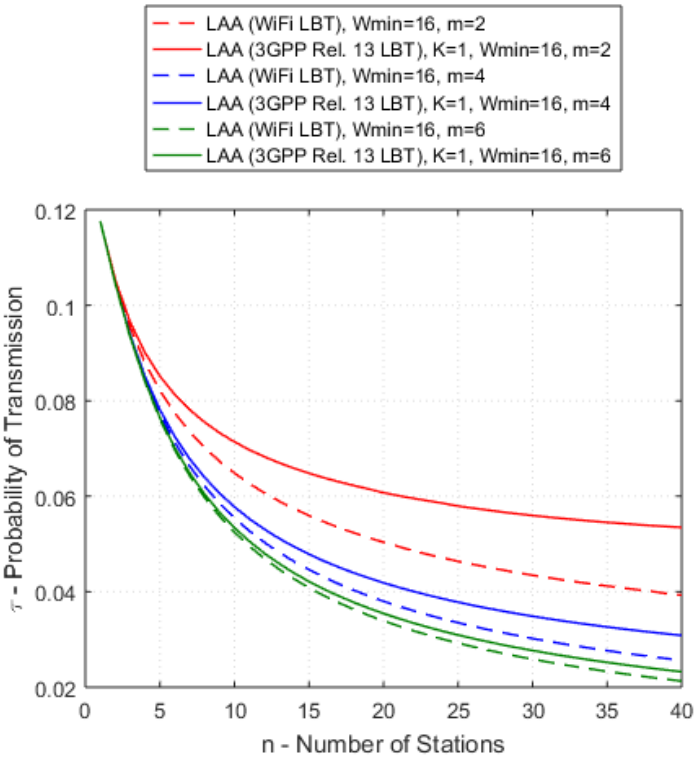

Figure 3.4: LAA vs. Wi-Fi Probability of Transmissions (Homogeneous Network)

sion probability, which in turn will cause more collisions and reduce throughput. However, this phenomenon only occurs when all n contending nodes are using the same LAA-LBT mechanism. Thus, it can be concluded that a dense homogeneous network consisting of LAA-LTE stations operating the LTE-LAA LBT mechanism will experience increased collisions. This is further evident in figure 3.3 which demonstrates that by increasing the value of $K = [1, 2, 4, 5, 8, 16]$, the probability of transmission decreases and the saturation throughput increases until it approaches Wi-Fi LBT throughput at around $K = 16$ to a negligible difference. It is noted however, that $K = 8$ is the maximum permitted value in the specification. In contrast, an LAA-LTE node will stand to gain an advantage when it finds itself amongst n contending Wi-Fi nodes due to the increased

transmission probability it solely gains. In essence, the K parameter added in the final specification provides an LTE-LAA eNB operator with the agility to coexist in both homogeneous and heterogeneous networks. By setting K=1, the LAA eNB benefits from an increased probability of transmission over co-channel neighboring Wi-Fi stations (heterogeneous network operation). Setting K=8 prevents co-channel collocated eNBs (homogeneous network operation) from degrading throughput.

K-Parameter and Initial Contention Window Size:

In addition, we examine the joint effect of the K-parameter and the initial contention window size on saturation throughput. For this we consider two LTE-LAA networks comprised of contrasting node densities. We plot the initial contention window size vs. normalized saturation throughout for $K \in [1, 3, 5, 8]$. We observe in figures 3.5 and 3.6 that for a dense LAA network (i.e. $n = 30$), and for smaller contention window size values, there is an increasing affect for the K parameter setting opposed to that of a less dense (e.g. sparse) network. However, we observe that the initial contention window size has a much more significant effect on the LTE-LAA LBT performance for both cases. Furthermore, we observe that there exists an optimal contention window size that yields maximum saturation throughput per network density. Therefore, LAA stations utilizing the standardized LTE-LAA LBT mechanism can achieve considerable performance gain by passively detecting the number of co-channel operating nodes and optimizing the initial contention window size along with the K parameter setting.

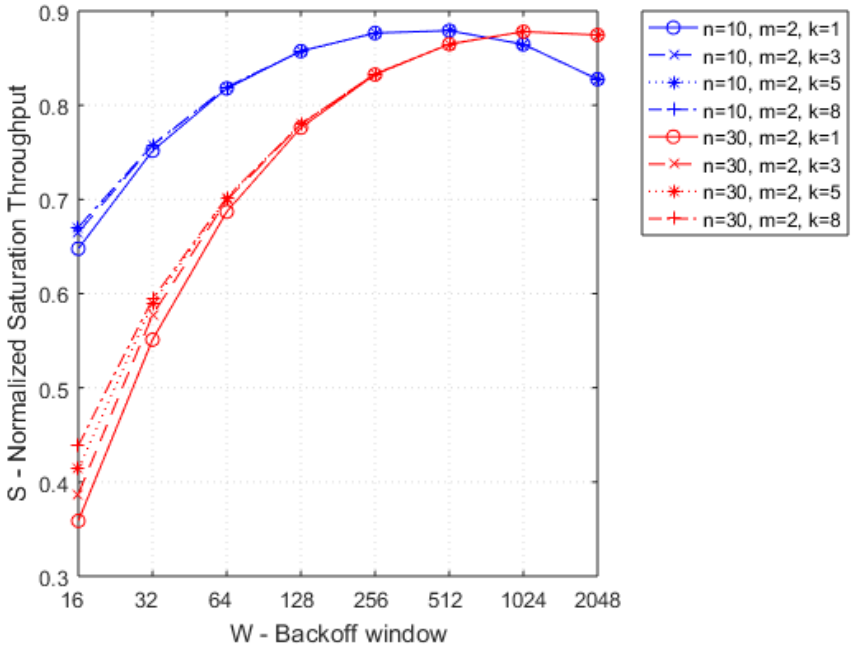

Figure 3.5: Normalized Saturation Throughput vs. Initial Contention Window Size ($n \in [10, 30], m = 2, k \in [1, 3, 5, 8]$)

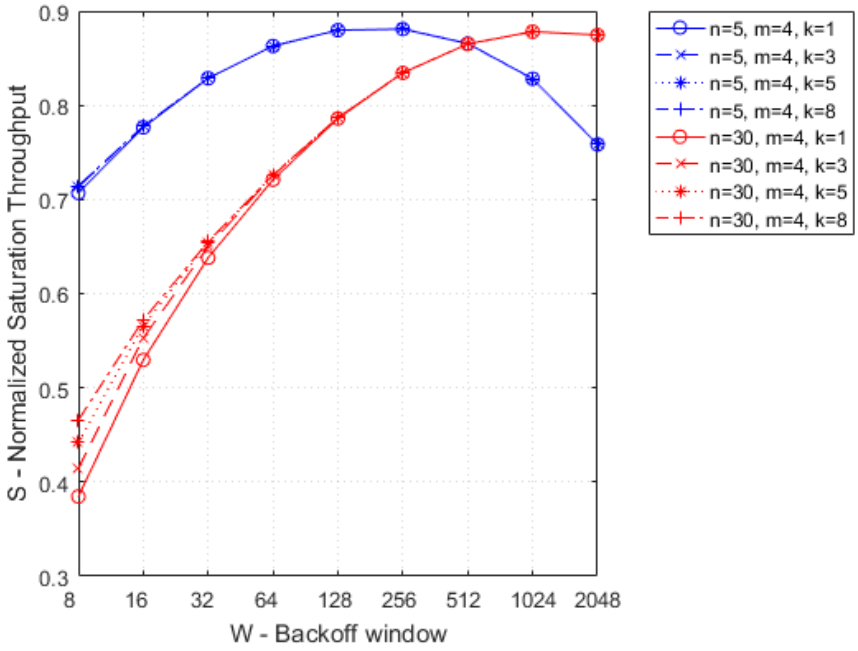

Figure 3.6: Normalized Saturation Throughput vs. Initial Contention Window Size ($n \in [5, 30], m = 4, k \in [1, 3, 5, 8]$)

K-Parameter and Transmission Occupancy Time:

Considering the transmission occupancy time and its effect on the saturation throughput of the LAA network. We observe in figures 3.7 and 3.8 that the saturation throughput increases as a function of the occupancy time. We note that the effect of the K parameter is greater on larger network sizes as compared to less dense and more sparse networks. Similarly, we also note that higher K parameter values improve performance for dense homogeneous LAA networks and that low priority class valued traffic (i.e. high priority p number) is less affected by optimizing K, in contrast to high priority traffic (i.e. low priority p value).

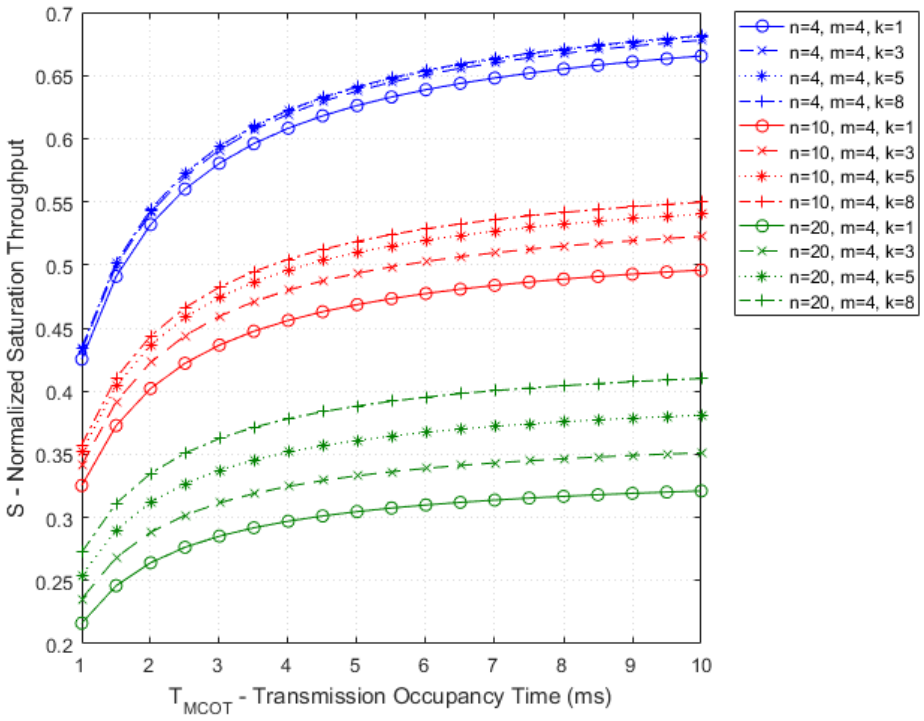

Figure 3.7: Normalized Saturation Throughput vs. Transmission Occupancy Time ($W = 4$, priority $p = 1$)

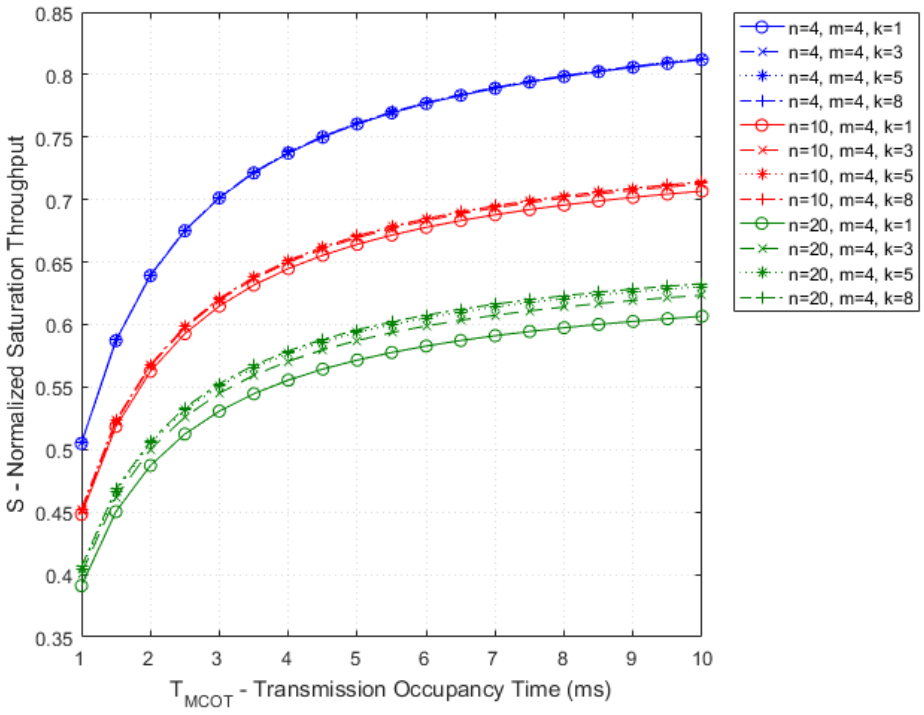

Figure 3.8: Normalized Saturation Throughput vs. Transmission Occupancy Time ($W = 16$, priority $p = 4$)

Figures 3.9 and 3.10 plot the joint function of the initial contention window size, transmission occupancy time and normalized saturation throughput. As the saturation throughput monotonically increases with respect to the transmission occupancy, we observe that the optimal solution will always lie on the highest occupancy time allowed. However, we observe that that user density and initial contention window size are quasi concave, and thus optimizing saturation throughput need only consider these two factors while maintaining maximum occupancy time.

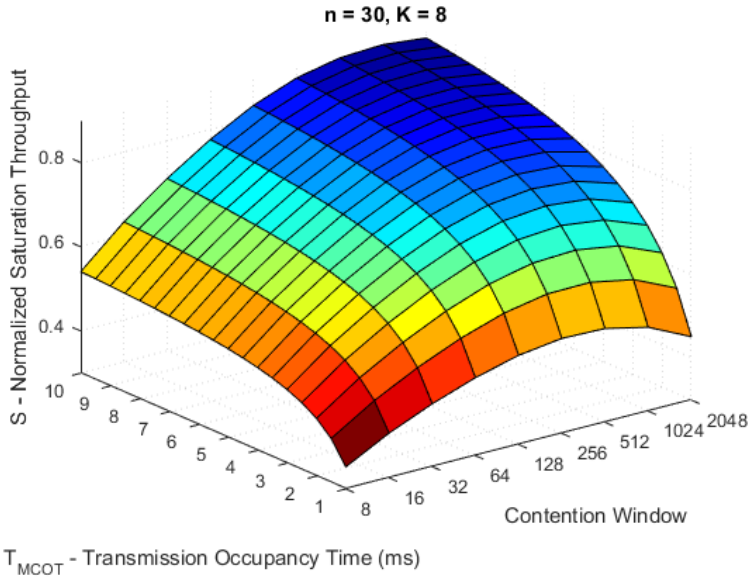

Figure 3.9: Normalized Saturation Throughput vs. Transmission Opportunity vs. Initial Contention Window Size $n = 30, K = 8$

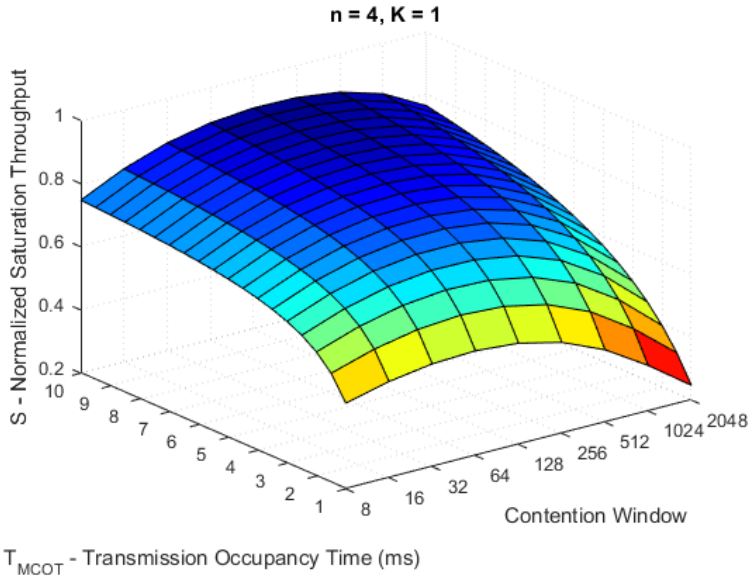

Figure 3.10: Normalized Saturation Throughput vs. Transmission Opportunity vs. Initial Contention Window Size $(n = 4, K = 1)$

K Parameter, Number of Stations and Initial Contention Window Size:

Plotting the normalized saturation throughput as function of the number of stations and the initial contention window size, for $K = [1, 8]$, we observe in fig-

ures 3.11 and 3.12 that the K value improves total saturation throughout, while continually shifting the optimal solution towards higher values of the initial contention window size, as the number of nodes in the network increase. Therefore, joint optimization of the K parameter, number of LAA nodes, Number of Wi-Fi nodes and Initial contention window size allow peak performance to be achieved in terms of saturation throughput.

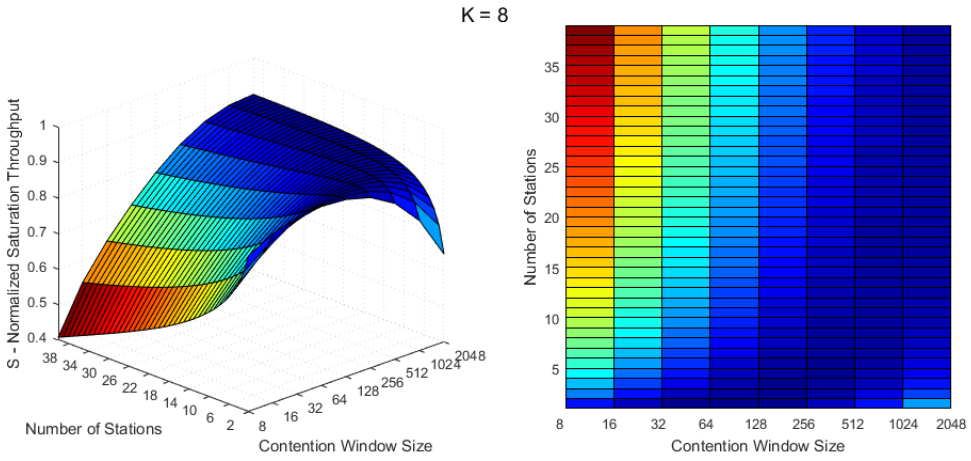

Figure 3.11: Normalized Saturation Throughput vs. Number of Stations vs. Initial Contention Window Size (K=8)

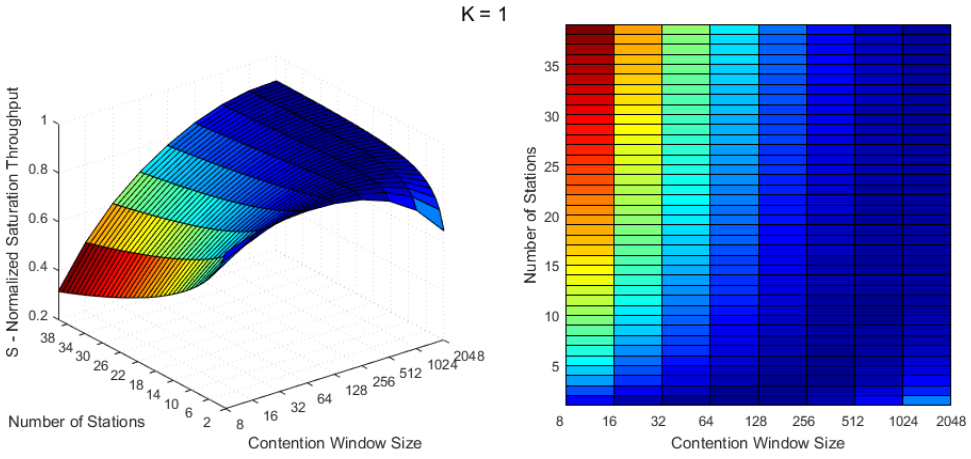

Figure 3.12: Normalized Saturation Throughput vs. Number of Stations vs. Initial Contention Window Size (K=1)

Chapter 4

Coexistence Performance Analysis

In this section we examine the coexistence performance of a standardized LTE-LAA homogeneous and heterogeneous network comprised of eNB stations operating the LTE-LAA LBT mechanism. We begin by deriving probability expressions for heterogeneous network operation. We then incorporate these newly derived expressions along with the previously derived homogeneous formulas in our coexistence performance analysis.

We assume a heterogeneous network consists of n_w Wi-Fi APs and n_l LTE-LAA eNB stations, all which are co-channeling and co-located, each with a full buffer. We consider only the DL transmission for one client per AP/eNB, implying the contention is between only the APs and eNBs. τ_w and τ_l denote the transmission probability of Wi-Fi and LTE-LAA respectively. From equation (3.12) we employ the derived transmission probability for LTE-LAA, and from equation (3.15) we obtain the probability of transmission for Wi-Fi. Accordingly, for the network consisting of n_w APs and n_l eNBs, the collision probability of a Wi-Fi AP transmitting with at least one of the other remaining $(n_w - 1)$ APs and n_l eNB stations can be given as:

$$P_w = 1 - (1 - \tau_w)^{n_w - 1} \cdot (1 - \tau_l)^{n_l}. \tag{4.1}$$

Similarly, the collision probability for an LTE-LAA eNB with at least one of the other remaining $(n_l - 1)$ eNBs and n_w Wi-Fi APs can be given by:

$$P_l = 1 - (1 - \tau_l)^{n_l - 1} \cdot (1 - \tau_w)^{n_w}. \tag{4.2}$$

We can now solve (3.12), (3.15), (4.1) and (4.2) jointly using numerical methods to compute the values of P_w, P_l, τ_w, and τ_l, respectively.

The transmission Probability of a Wi-Fi AP under this heterogeneous setup is the probability that at least one of the n_w APs transmit a packet during a time slot. This can be given by the probability:

$$P_{trw} = 1 - (1 - \tau_w)^{n_w}. \tag{4.3}$$

Similarly, the transmission Probability of an LTE-LAA eNB is the probability that at least one of the n_l eNBs transmit during a time slot. This probability can be given by:

$$P_{trl} = 1 - (1 - \tau_l)^{n_l}. \tag{4.4}$$

Using (4.3) and (4.4) we can now express the probability of successful transmission per station type:

For Wi-Fi, the probability of successful transmission is the probability that exactly one of the n_w Wi-Fi APs and non of the n_l LTE-LAA eNBs makes a transmission attempt in a given time slot. This can be expressed as:

$$P_{sw} = \frac{n_w \tau_w (1-\tau_w)^{n_w-1}(1-\tau_l)^{n_l}}{P_{trw}}. \tag{4.5}$$

Similarly for LTE-LAA, the probability of successful transmission is the probability that exactly one of the n_l eNBs and non of the n_w Wi-Fi stations makes a transmission attempt in a given time slot. This can be expressed as:

$$P_{sl} = \frac{n_l \tau_l (1-\tau_l)^{n_l-1}(1-\tau_w)^{n_w}}{P_{trl}}. \tag{4.6}$$

LTE and Wi-Fi use different modulation and coding schemes (MCS). During operation and transmission, and in a coexistence scenario, any given eNB or AP will change their MCS adaptively according to the channel state information, so their transmission rate will be dynamic. Assessing coexistence fairness by including system specific achievable bitrate, introduces an imbalance between the actual channel usage time of the two systems, and therefore results in imprecise interpretation of coexistence fairness. Assessing modulation or coding efficiency of both systems is not the subject and beyond the scope of this work. Therefore, to realize fairness of channel occupancy between the two systems, we assume both have equal bitrate, and express the saturation throughput in terms of the ratio of successful transmission time to the total channel time. Thus, we assume that both systems have equal efficiency when capturing the channel. We can now

express the saturation throughput for Wi-Fi as:

$$T_{put_w} = \frac{P_{trw} P_{sw} D_w}{T_{state}}, \tag{4.7}$$

and the saturation throughput of LAA can be expressed as:

$$T_{put_l} = \frac{P_{trl} P_{sl} D_l}{T_{state}}. \tag{4.8}$$

Here $D_w = \frac{PacketSize}{Bitrate} = D_l = T_{mcot,p}$. T_{state} is the normalizing condition which accounts for every possible scenario that can occur over the channel. It is given by the expression of (4.9)

$$\begin{gathered}
Tstate = (1 - P_{trw})(1 - P_{trl})\sigma + ... \\
P_{trw} P_{sw} (1 - P_{trl}) T_{ws} + ... \\
P_{trl} P_{sl} (1 - P_{trw}) T_{ls} + ... \\
P_{trw} (1 - P_{sw})(1 - P_{trl}) T_{wc} + ... \\
P_{trl} (1 - P_{sl})(1 - P_{trw}) T_{lc} + ... \\
P_{trw} P_{sw} P_{trl} P_{sl} T_a + ... \\
P_{trw} P_{sw} P_{trl} (1 - P_{sl}) T_a + ... \\
P_{trw} (1 - P_{sw}) P_{trl} P_{sl} T_a + ... \\
P_{trw} (1 - P_{sw}) P_{trl} (1 - P_{sl}) T_a.
\end{gathered} \tag{4.9}$$

σ is the time slot duration. T_{ws} is the duration of time the channel was sensed busy due to a successful transmission of Wi-Fi. T_{ls} is the duration of time the channel was sensed busy due to a successful transmission of LTE-LAA. T_{wc} is the

duration of time the channel was sensed busy due to a collision transmission of Wi-Fi. T_{lc} is the duration of time the channel was sensed busy due to a collision transmission of LTE-LAA. T_a is the duration of time the channel was sensed busy due to an inter-network transmission between Wi-Fi and LTE-LAA and is given as the larger timer between both.

The following subsections will present the coexistence performance under both network scenarios. However, to obtain a greater understanding of the coexistence performance of the underlying LBT mechanism of LTE-LAA, subsection (4.1) will analyze coexistence performance by setting equal parameter values to both network types. This follows the same thought process developed in chapter during performance analysis. The objective is to once more isolate the effect of all parameters except the underlining LBT mechanism in operation under heterogeneous co-channel mode, which allows us to identify the affect of the standardized LBT mechanism itself on the performance metric investigated. After that, subsection (4.2) proceeds to perform the analysis using standard specified parameters for each system, exploiting signaling and transmission chracteristics of LTE-LAA in the unlicensed band, exploring different priority classes defined in the standard, and depicting the coexistence performance of each system. Conclusively, we identify when an LTE-LAA eNB will obtain an advantage over Wi-Fi co-located and co-channeling AP stations.

4.1 Equal Parameter Coexistence for LTE-LAA and Wi-Fi

For equations (4.7) and (4.8), T_{state} contains the timers for a successful transmission and collision events. For Wi-Fi these expressions can be given as:

$$T_{wc} = (H + EP)/b_r + \delta + DIFS \tag{4.10}$$

$$T_{ws} = (H + EP)/b_r + \delta + SIFS + ACK + \delta + DIFS \tag{4.11}$$

In this equal parameter coexistence analysis examination, we assume LTE-LAA utilizes the same timer durations as Wi-Fi (i.e. $T_{wc} = T_{lc}$ and $T_{ws} = T_{ls}$). The parameters values of equations (4.10) and (4.11) are listed in table 4.1.

Figure 4.1 illustrates the total normalized saturation throughput, and the throughput achieved per network type. The number of heterogeneous nodes per network type are equal to half the number of nodes listed in the x-axis. i.e. $n_l = n_w = n/2$. We observe that the total sum channel utilization throughput of the hetero-

Table 4.1: Channel Access Parameters for LTE-LAA Coexistence Analysis

Parameter	Unit
m_p	2
$CW_{p,min}$:	15
$T_{mcot,p}$: Maximum channel occupancy time	8ms
EP: Packet Payload	8kbits
br: bitrate	1Mbps
δ: Propagation Delay	$1\mu s$
H: Packet Header (PHY + MAC)	400bits
ACK: HARQ-ACK	240bits
σ: TimeSlot	$9\mu s$
DIFS:	$34\mu s$
T_d:	$16\mu s + (m_p + \sigma)$
SIFS	$16\mu s$
K Parameter	1

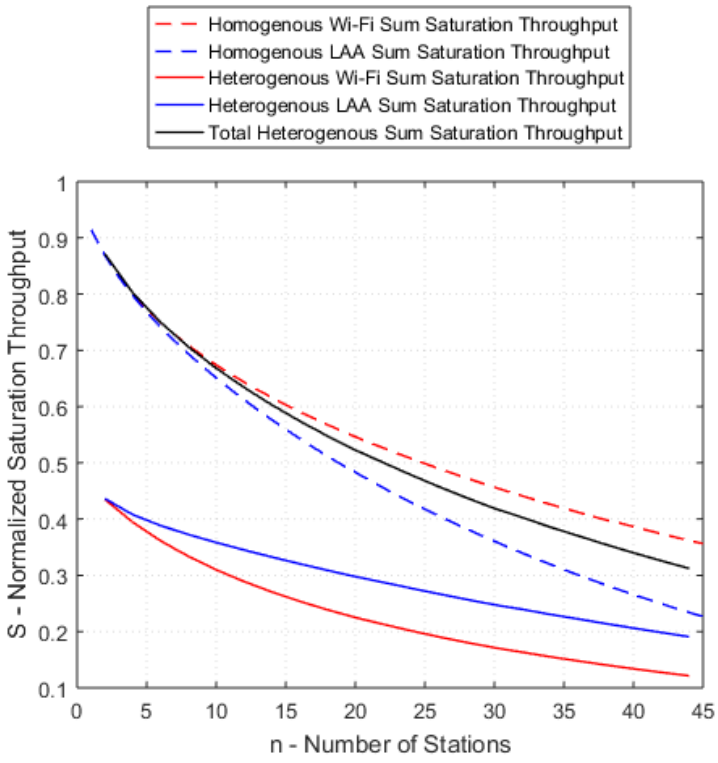

Figure 4.1: Normalized Saturation Throughput for an Equal Parameter Heterogeneous Network

geneous network is higher than a homogeneous network consisting of the same number of LTE-LAA eNBs (i.e. throughput 20eNBs + 20APs > throughput 40 eNBs). This can be attributed to the increasing collisions that occur in a dense homogeneous LTE-LAA network when K=1. However, we also observe the total throughput of the heterogeneous LTE-LAA network exceeds that of Wi-Fi as the number of nodes increase. This occurs due to the increasing number of collisions happening as more nodes are introduced into the network. As more collisions occur, Wi-Fi retains a higher backoff stage increasing its backoff time, while LAA resets to a lower stage which results in an increased opportunity of capturing the channel and transmitting. This aligns with insights attained from the performance analysis part shown in section 3.4.1. Furthermore, it can be concluded that

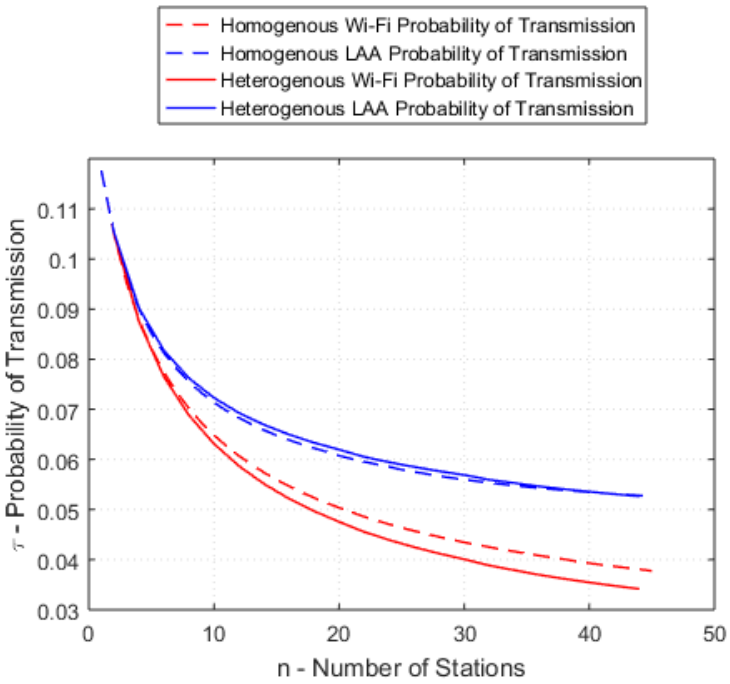

Figure 4.2: Probability of Transmission for an Equal Parameter Heterogeneous Network

the LBT mechanism of LTE-LAA does provide an advantage over Wi-Fi when all other parameters are equal. Results are confirmed when we observe figure 4.2 illustrating the probability of transmission for both networks in heterogeneous operation. We see that LTE-LAA's transmission probability marginally increases above the homogeneous network case, whereas Wi-Fi's transmission probability somewhat decreases below its homogeneous counterpart. Nevertheless, in all cases, LTE-LAA retains a higher transmission probability over Wi-Fi.

4.2 Standardized Parameter Coexistence for LTE-LAA and Wi-Fi

In this subsection we conduct heterogeneous coexistence analysis under the standard specific parameter settings of each network type. Moreover, for the analysis to be complete, we note the following considerations, characteristic of LTE-LAA, which are to be taken into account in the analysis:

1. Upon completing the channel access procedures and capturing the channel, the eNB can continuously transmit on a carrier on which the LAA Scell transmissions are to be performed for $t_{mcot,p}$ as shown in table 2.2 for each priority class. This transmission opportunity can be up to 8ms for priority class 4, and 10ms if the absence of any other technology sharing the carrier can be guaranteed on a long term basis (e.g. by level of regulation). Therefore, under saturation and ideal channel conditions assumed, the eNB will utilize its full transmission opportunity.

2. A new frame structure type 3 is applicable to LAA. Each radio frame is 10 ms long and consists of 10 subframes of length 1 ms. Any of these 10 subframes can be used for uplink/downlink transmission or can be empty. LAA transmission can start and end at any subframe and can consist of one or more consecutive subframes in the burst. LAA downlink transmission can start from the 0th Orthogonal Frequency Division Multiplexing (OFDM) symbol (Subframe boundary) or from the 7th OFDM symbol (Second Slot Starting Position) of a subframe. LAA downlink transmission can either end at the subframe boundary or at any of the Downlink Pilot Time Slot (DwPTS) symbols. Therefore, the last subframe can be completely occupied

with 14 OFDM symbols or can consist of any of DwPTS duration symbols. Figure 4.3 depicts this new frame structure type 3, the slot boundaries and DwPTS duration symbols.

3. Once transmission is complete, the receiver transmits the acknowledgment through the licensed band if the symbols are successfully decoded. A reference subframe which is the starting subframe of the most recent transmission on the carrier made by the eNB, for which at least some HARQ-ACK feedback is expected to be available is considered for assessing retransmissions. Thus, the minimum resolution of a data re-transmission and the collision time in LTE-LAA is one sub frame.

With the assumption of saturation and ideal channel conditions, an upper boundary can be set for the number of subframes transmitted. (e.g. the maximum number of subframes that can be transmitted for priority class 4 is 8 sub frames, each 1ms). Therefore, when an LTE-LAA eNB captures and successfully transmits, the duration of time the channel is sensed busy can be expressed as:

$$T_{ls} = T_{mcot,p} + \delta + T_d \tag{4.12}$$

$T_{mcot,p}$ is the TxOP of the LTE-LAA (8ms for p=4). This indicates that once the eNB captures the channel, it will saturate the channel for the total amount of time ($T_{mcot,p}$) that it is allowed. T_d is the standard specified sensing time equivelent to DIFS for Wi-Fi. δ and T_d can be found in table 4.1. The duration of time the channel is sensed busy when an LTE-LAA eNB transmission experiences collision under saturation and ideal channel conditions is expressed as:

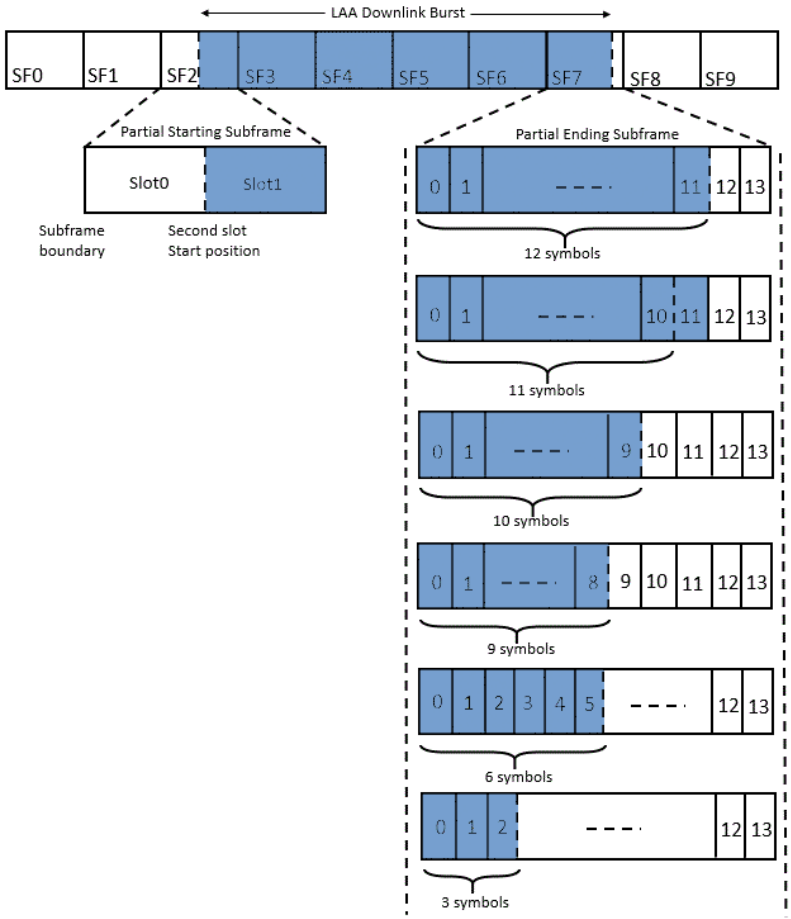

Figure 4.3: LTE-LAA frame 3 structure

$$T_{lc} = T_{subframe} + \delta + T_d \tag{4.13}$$

$T_{subframe} = 1ms$.

Using the above derived expressions, we proceed to analyze different coexistence cases pertaining to different priority classes as defined in the standard:

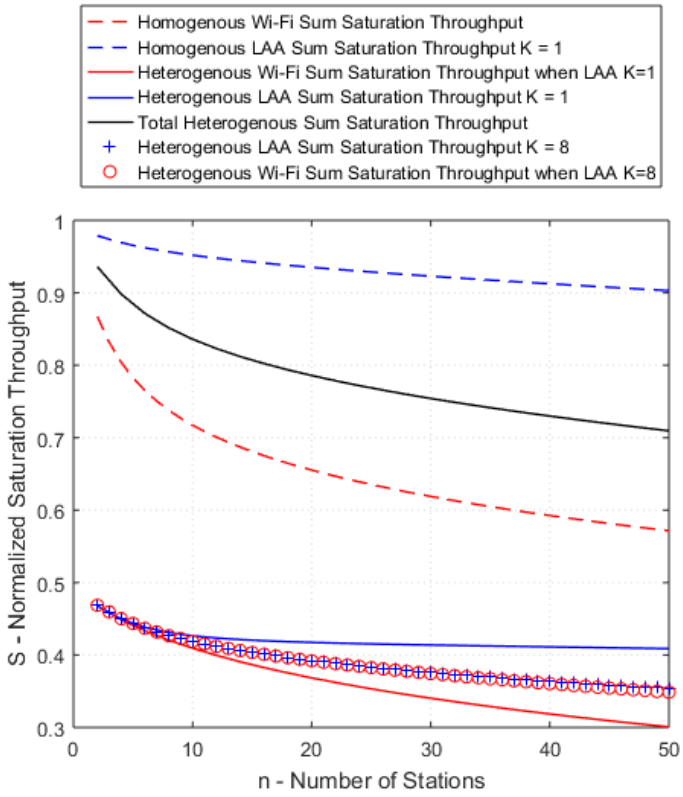

Figure 4.4: LAA Priority = 4, $m_p = 7$, $m_{wifi} = 7$ and contention window steps W $\in$ [15,31,63,127,255,511,1023]

4.2.1 LAA Priority 4 and Priority 3

For priority class $p = 4$, the standard defines contention window steps W $\in$ [15,31,63,127,255,511,1023], number of contention stages $m_p = 7$, and transmission opportunity duration of $T_{mcot,p} = 8ms$. Figure 4.4 depicts coexistence performance results attained for this priority class. We first observe that under standardized parameters, the saturation throughput of homogeneous coexistence operation achieved in LTE-LAA eNBs is comparatively higher than that of Wi-Fi APs for all network densities. This is attributed to two factors:

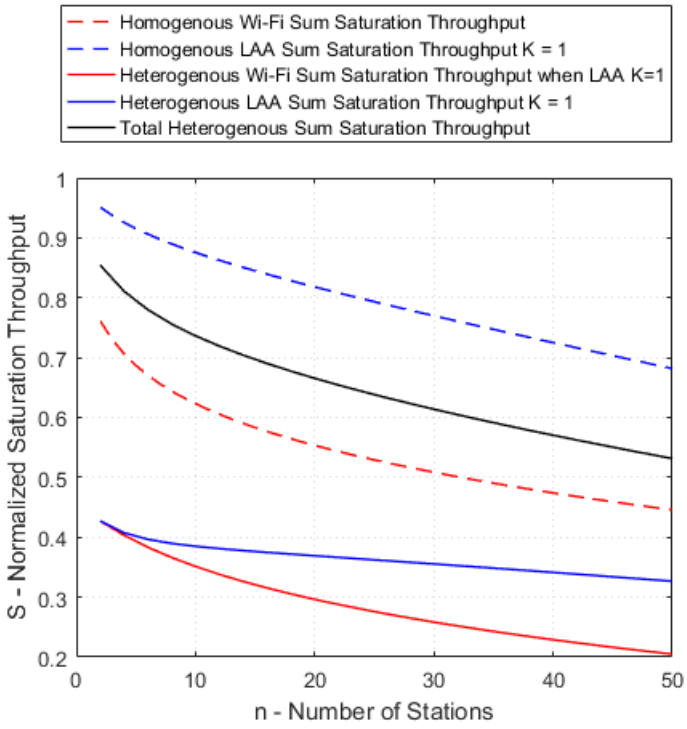

Figure 4.5: LAA Priority = 3, $m_p = 3$, $m_{wifi} = 3$ and contention window steps W $\in$ [15,31,63]

1. The use of the licensed band for sending HAQR-ACK messages which allows for increased channel utilization of the unlicensed band.

2. The increased efficiency attained from the larger successful transmission time opposed to the reduced collision time occurring over the minimum resolution time of LTE-LAA.

However, this performance difference between LTE-LAA and Wi-Fi at smaller node numbers disappears under the heterogeneous network scenario. This occurs because the collision time increases to that of the higher of both networks, as can be seen in the T_{state} expression found in equation (4.7) and (4.8).

Additionally, despite the unfavorable effect that Wi-Fi's collision time has on

channel utilization, we observe that LTE-LAA continually achieves increasing throughput as the number of nodes in the system increases. This occurs strictly due to the LAA LBT mechanism itself, confirming the insights we obtained in chapter 3. As the number of nodes increases, the number of collisions increase, which causes Wi-Fi AP stations to retransmit at the higher contention stages, whereas LAA eNBs reset to the starting stage, gaining an increased transmission opportunity. Furthermore, we also observe in figure 4.4 that the total heterogeneous sum saturation throughput of the system is higher than homogeneous Wi-Fi, which occurs due to LTE-LAA's increased channel utilization and efficiency.

Finally, we observe in figure 4.4 that by setting K=8, the saturation throughput and performance of LTE-LAA almost matches Wi-Fi to a negligible difference confirming the insights obtained in the performance analysis of the LBT mechanism presented chapter 3.

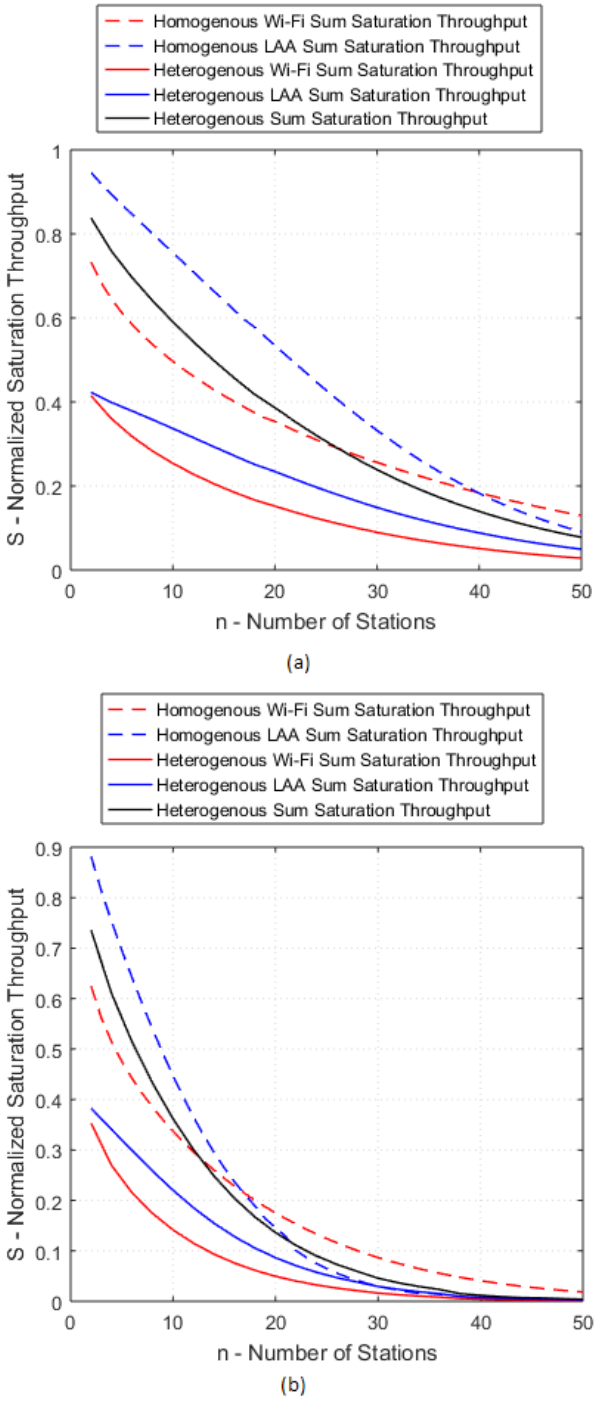

Figure 4.6: a) LAA Priority = 2, $m_p = 1$, $m_{wifi} = 1$ and W $\in$ [7,15]. b) LAA Priority = 1, $m_p = 1$, $m_{wifi} = 1$ and W $\in$ [3,7]

4.2.2 LAA Priority 2 and Priority 1

For priority class $p = 2$, the standard defines W $\in$ [7,15], $m_p = 1$, and $T_{mcot,p} = 3ms$ and for priority class $p = 1$, the standard defines W $\in$ [3,7], $m_p = 1$, and $T_{mcot,p} = 2ms$. Figure 4.6 (a) and (b) depict the results attained for $p = 2$ and $p = 1$ respectively. We observe that LTE-LAA saturation throughput converges towards Wi-Fi's throughput in contrast to the diverging behaviour we observed for priority class 4. This is the result of a dual affect caused by the small contention window sizes and backoff stages for these priority classes. As the number of nodes increases, the higher saturation throughput attained from the increased transmission probability diminishes as a result of the increasing collisions occurring. We observe that even for a homogenous network, for priority 2, and around $n = 40$, the saturation throughput drops below that of Wi-Fi gradually lowering the improved channel utilization and efficiency that LTE-LAA was achieving over Wi-Fi. Likewise, we find this threshold dropping further for Priority $P = 1$, to around $n = 17$.

4.2.3 Single LAA Station

Lastly, to illustrate the gain a single LAA user achieves over incumbant Wi-Fi stations when operating under co-channel heterogeneous mode, we consider a scenario where one LAA eNB is amongst (n) Wi-Fi AP stations. By dividing the total sum saturation throughput per network type over the number of nodes, we compute the saturation throughput per network station. Figure 4.7 depicts the results attained. We observe for priority class 4, that the saturation throughput of an LTE-LAA station closely follows that of Wi-Fi regardless of the number of Wi-Fi nodes present. This is due to the large backoff stages, low density

of nodes present and low number of retransmissions occurring, resulting in an insignificant difference in performance. However, we observe for priority class 1 and 2, that an LTE-LAA station achieves slightly higher saturation throughput than Wi-Fi. This continually occurs despite the increasing number of Wi-Fi nodes present in the network. Therefore, we find that under the more commonly found low density heterogeneous networks, an LTE-LAA station achieves similar performance to Wi-Fi for priority class 4, and attains an advantage for higher priority classes (1,2 and 3).

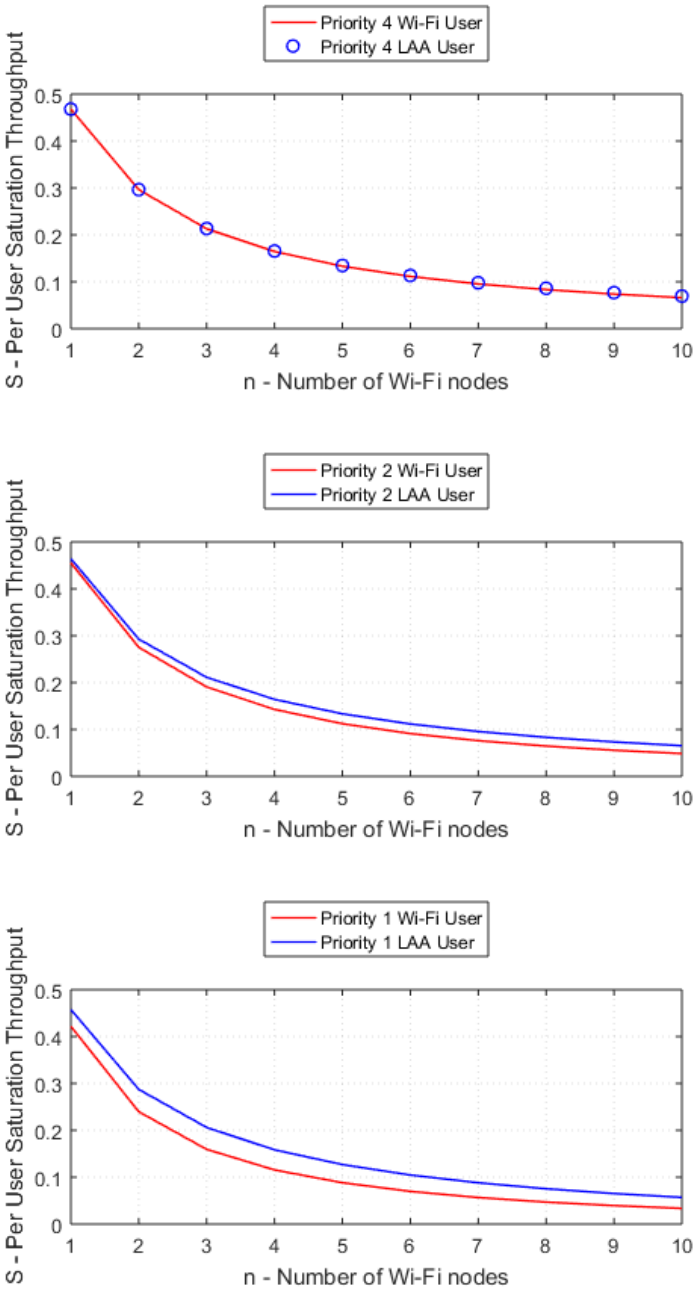

Figure 4.7: LAA Single Station Saturation Throughput for Priority Classes P = $\{4, 2, 1\}$.

Chapter 5

Conclusion and Future Work

5.1 Conclusion

The increase in mobile broadband traffic is expected to remain a trend for many years to come. This is mainly attributed to the ever changing mix and growth of wireless devices, the emergence of more demanding services, and the continually growing number of mobile wireless users. Consequently, as demand grows, a greater pressure is placed on radio access networks (RANs) to be able to meet the challenge of providing and guaranteeing an adequate level of Quality of service (QoS) to their users. Extending LTE to the Unlicensed band is expected to be a key enabler, amongst other candidate solutions, to alleviate the foreseen capacity challenge. Nevertheless, this extension poses significant challenges in regards to the coexistence of the LTE technology with current incumbents of the unlicensed band. Ultimately, LTE is expected to coexist with other unlicensed technologies in a "fair" manner. To this end, the recently 3GPP standardized technology, termed LTE License Assisted Access (LTE-LAA) is considerd to be a key facilitor for bringing LTE to the unlicensed spectrum. LTE-LAA adopts the tried-and-true mechanism of Listen-Before-Talk (LBT) as its method of coexistence. Described to fundamentally resemble the CSMA/CA of Wi-Fi, LTE-LAA

adopts a newly introduced K-parameter that governs the retransmission rate of the maximum contention stage of the LAA LBT mechanism. Building an analytical modeling framework that eliminates implementation biases which could arise in empirical experimentation, allows analyzing and evaluating the coexistence of the LTE-LAA technology in an accurate and transparent manner. This dissertation fills the gap. The dissertation addresses the issue of evaluating and modeling LTE-LAA's Listen-Before-Talk (LBT) mechanism and its effect on the coexistence of the technology in the unlicensed band effectively. The work presents a novel analytical model using Markov Chain that accurately models the 3GPP LTE-LAA LBT scheme, as specified in the 3rd Generation Partnership Project (3GPP) release 13 and 14 standard, which has been additionally adopted in the Multefire specification as well. Model validation is demonstrated through numerical and simulation analysis. By means of the proposed model, performance evaluation of the standardized LAA-LBT is examined. Furthermore, following model development, a comprehensive coexistence analysis study of both homogeneous and heterogeneous network scenarios involving LTE-LAA Evolved Node Bs (eNB) and Wi-Fi Access Points (APs) is examined and carried out. Results indicate:

1. The LTE-LAA LBT coexistence mechanism achieves a higher probability of transmission than the DCF mechanism of Wi-Fi.

2. The newly introducted K-Parameter serves as an optimization element that supports agility to the coexistence of LTE-LAA. Under heterogeneous operation (LTE coexisting with WiFi), lower values of K (e.g. K=1) favor LTE eNB over WiFi transmissions, while higher values of K (e.g. K=8) provide WiFi a fair oppurtunity for coexistence. Under homogeneous operation

(LTE only network), lower values of K increase contention and lower saturation throughout, while higher values of K improve network throughout performance.

3. Initial Contention window size was found to be a key optimization parameter to be considered jointly with the number of LAA and Wi-Fi collocated, and co-channeling stations.

4. A key performance advantage for LTE-LAA's LBT was identified at higher priority class traffic. The advantage was found to be in the range of [3 - 6]% increase in terms of saturation throughput for a single LTE-LAA station present amongst a single, and low number of Wi-Fi nodes.

5.2 Future Work and Potential Research Directions

The work presented in this dissertation serves as a bedrock for a thorough and objective look at the coexistence performance of the LTE-LAA technology. The performance of Wi-Fi and LTE-LAA stations in a coexistence system depends on the channel access parameters (e.g. Initial Contention window size, K-parameter, TxOP) adopted for each of these technologies. By changing these parameters, a considerable improvement in terms of higher per user throughput can be achieved. Future work incorporating the developed model will extend the work by investigating the optimization of LTE-LAA offloading under different constraints, including threshold adaptation for improved throughput performance, and transmission delay performance analysis.

Furthermore, it is noted, that continually emerging Wi-Fi specifications are adopting LTE enhancements to improve spectral efficiency and enhance throughput. One potential research direction is the investigation of a tractable analytical

LBT model under non-saturation and non-ideal transmission channel characteristics for Orthogonal Frequency Division Multiple Access (OFDMA) enabled transmissions. Another interesting research direction is the investigation of the mutual interference of heterogeneous LTE-LAA and Wi-Fi networks under different spatial distribution point process models using stochastic geometry, taking into account varying levels of energy detection thresholds. Finally, the investigation of coexistence distributed sensing along with new MAC and PHY modes capable of supporting enhanced throughput remains an open research problem and could result in a paradigm changing outcome on the coexistence performance of unlicensed band incumbents.

Bibliography

[1] Cisco white paper, "Cisco Visual Networking Index: global mobile data traffic forecast update, 2016–2021," [Online]. Available: https://www.cisco.com/c/en/us/solutions/collateral/service-provider/visual-networking-index-vni/mobile-white-paper-c11-520862.pdf.

[2] B. Romanous, N. Bitar, A. Imran and H. Refai, *"Network densification: Challenges and opportunities in enabling 5G,"*. 2015 IEEE 20th International Workshop on Computer Aided Modelling and Design of Communication Links and Networks (CAMAD), Guildford, 2015, pp. 129-134.

[3] O. G. Aliu, A. Imran, M. A. Imran and B. Evans, *"A Survey of Self Organisation in Future Cellular Networks,"*. in IEEE Communications Surveys & Tutorials, vol. 15, no. 1, pp. 336-361, First Quarter 2013.

[4] N. Bitar, A. Imran and H. Refai, *"A user centric self-optimizing grid-based approach for antenna steering based on call detail records,"*. 2016 IEEE Wireless Communications and Networking Conference, Doha, 2016, pp. 1-6.

[5] A. Imran A. Zoha *"Challenges in 5G: how to empower SON with big data for enabling 5G"*. IEEE Network vol. 28 no. 6 pp. 27-33 Nov.-Dec. 2014.

[6] H. Lee, S. Vahid and K. Moessner, *"A Survey of Radio Resource Management for Spectrum Aggregation in LTE-Advanced,"*. in IEEE Communications Surveys & Tutorials, vol. 16, no. 2, pp. 745-760, Second Quarter 2014.

[7] S. Rangan, T. S. Rappaport and E. Erkip, *Millimeter-Wave Cellular Wireless Networks: Potentials and Challenges,*. in Proceedings of the IEEE, vol. 102, no. 3, pp. 366-385, March 2014.

[8] M. Jaber, M. A. Imran, R. Tafazolli and A. Tukmanov, *"5G Backhaul Challenges and Emerging Research Directions: A Survey,"*. in IEEE Access, vol. 4, pp. 1743-1766, 2016.

[9] Qualcomm Incorporated, "Extending LTE advanced to unlicensed spectrum," [Online]. Available: https://www.qualcomm.com/media/documents/files/white-paper-extending-lte-advanced-to-unlicensed-spectrum.pdf. Accessed May 2018.

[10] HUAWEI, "U-LTE: unlicensed spectrum utilization of LTE, 2014," [Online]. Available: www.huawei.com/ilink/en/download/HW_327803.

[11] Ericsson, "LTE license assisted access," [Online]. Available: https://web.archive.org/web/20161014143936/http://www.ericsson.com/res/thecompany/docs/press/media_kits/ericsson-license-assisted-access-laa-january-2015.pdf. Accessed May 2018.

[12] Qualcomm Incorporated, "Introducing multefire: LTE-like performance with Wi-Fi like simplicity," [Online]. Available: https://www.qualcomm.com/news/onq/2015/06/11/introducing-multefire-lte-performance-wi-fi-simplicity. Accessed May 2018.

[13] N. Rupasinghe and İ. Güvenç, "Licensed-assisted access for WiFi-LTE coexistence in the unlicensed spectrum," 2014 IEEE Globecom Workshops (GC Wkshps), Austin, TX, 2014, pp. 894-899.

[14] Y. Jian, C. F. Shih, B. Krishnaswamy and R. Sivakumar, "Coexistence of Wi-Fi and LAA-LTE: Experimental evaluation, analysis and insights," 2015 IEEE International Conference on Communication Workshop (ICCW), London, 2015, pp. 2325-2331.

[15] S. Xu, Y. Li, Y. Gao, Y. Liu and H. Gačanin, "Opportunistic Coexistence of LTE and WiFi for Future 5G System: Experimental Performance Evaluation and Analysis," in IEEE Access, vol. 6, pp. 8725-8741, 2018.

[16] A. M. Cavalcante, *"Performance evaluation of LTE and Wi-Fi coexistence in unlicensed bands,"*. in Proc. IEEE 77th Veh. Technol. Conf. (VTC Spring), Dresden, Germany, Jun. 2013, pp. 1–6.

[17] T. Nihtilä et al., *"System performance of LTE and IEEE 802.11 coexisting on a shared frequency band,"* . 2013 IEEE Wireless Communications and Networking Conference (WCNC), Shanghai, 2013, pp. 1038-1043.

[18] F. M. Abinader et al., *"Enabling the coexistence of LTE and Wi-Fi in unlicensed bands,"*. IEEE Commun. Mag., vol. 52, no. 11, pp. 54–61, Nov. 2014.

[19] *https://web.archive.org/web/20170316191518/http://www.lteuforum.org/.*

[20] Qualcomm, *"LTE in unlicensed spectrum: Harmonious coexistence with WiFi"*. White Paper, Qualcomm, San Jose, CA, USA, 2012. [Online]. Available: https://www.qualcomm.com/media/documents/files/lte-unlicensed-coexistence-whitepaper.pdf

[21] Mukherjee, et al., *"System Architecture and Coexistence Evaluation of Licensed-Assisted Access LTE with IEEE 802.11,"*. IEEE ICC Workshop, pp. 2350-2355, London, UK, 8-12 June 2015.

[22] Y. Song, K. W. Sung and Y. Han, *"Coexistence of Wi-Fi and Cellular With Listen-Before-Talk in Unlicensed Spectrum,"* . in IEEE Communications Letters, vol. 20, no. 1, pp. 161-164, Jan. 2016.

[23] C. Chen, R. Ratasuk, and A. Ghosh, *"Downlink Performance Analysis of LTE and WiFi Coexistence in Unlicensed Bands with a Simple Listen-before-talk Scheme,"* . IEEE VTC Spring, pp. 1-5, Glasgow, Scotland, 11-14 May 2015.

[24] R. Yin, G. Yu, A. Maaref, and Y. Li, *"Adaptive LBT for Licensed Assisted Access LTE Networks,"* . IEEE Globecom, pp. 1-6, San Diego, US, 6-10 Dec. 2015.

[25] S. Saadat, D. Chen, K. Luo, M. Feng and T. Jiang, *"License assisted access-WiFi coexistence with TXOP backoff for LTE in unlicensed band,"* . in China Communications, vol. 14, no. 3, pp. 1-14, March 2017.

[26] Y. Li, T. Zhou, Y. Yang, H. Hu and M. Hamalainen, *"Fair Downlink Traffic Management for Hybrid LAA-LTE/Wi-Fi Networks,"* . in IEEE Access, vol. 5, no. , pp. 7031-7041, 2017.

[27] T. Tao, F. Han and Y. Liu, *"Enhanced LBT algorithm for LTE-LAA in unlicensed band,"*. 2015 IEEE 26th Annual International Symposium on Personal, Indoor, and Mobile Radio Communications (PIMRC), Hong Kong, 2015, pp. 1907-1911.

[28] V. Mushunuri, B. Panigrahi, H. K. Rath and A. Simha, *"Fair and Efficient Listen Before Talk (LBT) Technique for LTE Licensed Assisted Access (LAA) Networks,"* . 2017 IEEE 31st International Conference on Advanced Information Networking and Applications (AINA), Taipei, 2017, pp. 39-45.

[29] Wang J, Du J, Xu J, Wu H. *"Harmonious coexistence solution between stand-alone LTE andWiFi in unlicensed band"*. Trans Emerging TelTech. 2017;e3155.https://doi.org/10.1002/ett.3155

[30] A. Bhorkar, C. Ibars, A. Papathanassiou and P. Zong, *"Medium access design for LTE in unlicensed band,"* . 2015 IEEE Wireless Communications and Networking Conference Workshops (WCNCW), New Orleans, LA, 2015, pp. 369-373.

[31] H. Wang, M. Kuusela, C. Rosa, and A. Sorri, *"Enabling Frequency Reuse for Licensed-Assisted Access with Listen-before-talk in Unlicensed Bands,"* . IEEE VTC Spring, pp. 1-5, Nanjing, China, 15-18 May 2016

[32] Q. Chen, G. Yu, A. Maaref, Y. Li, and A. Huang, *"Rethinking Mobile Data Offloading for LTE in Unlicensed Spectrum,"* . IEEE Transactions on Wireless Communications, vol. 15, no. 7, pp. 4987-5000, July 2016

[33] Study on Licensed-Assisted Access to Unlicensed Spectrum, 3GPP TR 36.889 V13.0.0 (2015-06).

[34] H. J. Kwon et al., *"Licensed-Assisted Access to Unlicensed Spectrum in LTE Release 13,"*. in IEEE Communications Magazine, vol. 55, no. 2, pp. 201-207, February 2017. doi: 10.1109/MCOM.2016.1500698CM

[35] Q. Cui, Y. Gu, W. Ni and R. P. Liu, *"Effective Capacity of Licensed-Assisted Access in Unlicensed Spectrum for 5G: From Theory to Application,"*. in IEEE Journal on Selected Areas in Communications, vol. 35, no. 8, pp. 1754-1767, Aug. 2017.

[36] J. Yi, W. Sun, S. Park and S. Choi, *"Performance Analysis of LTE-LAA Network"*. in IEEE Communications Letters, vol. PP, no. 99, pp. 1-1. doi: 10.1109/LCOMM.2017.2779752

[37] J. Zhang, M. Wang, M. Hua, T. Xia, W. Yang and X. You, *"LTE on License-Exempt Spectrum,"*, in IEEE Communications Surveys & Tutorials, vol. 20, no. 1, pp. 647-673, Firstquarter 2018.

[38] Evolved Universal Terrestrial Radio Access (E-UTRA) Physical layer procedures, 3GPP TS 36.213 V13.6.0 (2017-06).

[39] S. Wang, Q. Cui and Y. Gu, *"Performance analysis of multi-carrier LAA and Wi-Fi coexistence in unlicensed spectrum,"*. 2017 IEEE/CIC International Conference on Communications in China (ICCC), Qingdao, 2017, pp. 1-5.

[40] Y. Zhang, Y. Chang and T. Zeng, *"Coexistence performance analysis of LAA based on release 13,"* 2017 International Symposium on Wireless Communication Systems (ISWCS), Bologna, 2017, pp. 90-95.

[41] O. El-Samadisy, M. Khedr and A. El-Helw, *"Performance Evaluation of MAC for IEEE 802.11 and LAA LTE,"* 2016 International Conference on Computational Science and Computational Intelligence (CSCI), Las Vegas, NV, 2016, pp. 923-928.

[42] Y. Gao, Q. Huang, S. Xu, H. Li, Z. Li and W. Tang, *"Experimental Performance Evaluation and Analysis of LAA and Wi-Fi Coexistence in the Unlicensed Spectrum,"* 2016 IEEE Globecom Workshops (GC Wkshps), Washington, DC, 2016, pp. 1-6.

[43] Y. Gao, X. Chu and J. Zhang, *"Performance Analysis of LAA and WiFi Coexistence in Unlicensed Spectrum Based on Markov Chain,"* 2016 IEEE Global Communications Conference (GLOBECOM), Washington, DC, 2016, pp. 1-6.

[44] X. Yan, H. Tian and C. Qin, *"A Markov-Based Modelling with Dynamic Contention Window Adaptation for LAA and WiFi Coexistence,"* 2017 IEEE 85th Vehicular Technology Conference (VTC Spring), Sydney, NSW, 2017, pp. 1-6.

[45] Z. Tang, X. Zhou, Q. Hu and G. Yu, *"Throughput Analysis of LAA and Wi-Fi Coexistence Network With Asynchronous Channel Access,"* in IEEE Access, vol. 6, pp. 9218-9226, 2018.

[46] W. Wang, P. Xu, Y. Zhang and H. Chu, *"Performance analysis of LBT Cat4 based downlink LAA-WiFi coexistence in unlicensed spectrum,"* 2017 9th International Conference on Wireless Communications and Signal Processing (WCSP), Nanjing, 2017, pp. 1-6.

[47] M. Mehrnoush, V. Sathya, S. Roy and M. Ghosh, *"Analytical Modeling of Wi-Fi and LTE-LAA Coexistence: Throughput and Impact of Energy Detection Threshold"* [Online]. Available: https://arxiv.org/pdf/1803.02444.pdf

[48] IEEE Standard for Information technology–Telecommunications and information exchange between systems Local and metropolitan area networks–Specific requirements - Part 11: *"Wireless LAN Medium Access Control (MAC) and Physical Layer (PHY) Specifications,"* in IEEE Std 802.11-2016 (Revision of IEEE Std 802.11-2012) , vol., no., pp.1-3534, Dec. 14 2016.

[49] *LTE-U: unlicensed spectrum utilization of LTE, Huawei White Paper, 2014"*. [Online]. Available: http://www.huawei.com/ilink/en/download/HW_327803. Accessed Jan 2019.

[50] N. Bitar, M. O. Al Kalaa, S. J. Seidman and H. H. Refai, *"On the Coexistence of LTE-LAA in the Unlicensed Band: Modeling and Performance Analysis,"*. in IEEE Access, vol. 6, pp. 52668-52681, 2018.

[51] Multefire Alliance, *"International Telecommunications Union (ITU)"*, [Online]. Available: https://www.itu.int/en/Pages/default.aspx. Accessed Jan 2019.

[52] nutsaboutnets, *"WifiEagle Single- and Dual-Band 802.11 Channel Analyzers"*, [Online]. Available: http://nutsaboutnets.com. Accessed Jan 2019.

[53] cablefree, *"802.11ac Technology"*, [Online]. Available: https://www.cablefree.net/ Accessed Jan 2019.

[54] Dusmantha Tennakoon, *"Unlicensed National Information Infrastructure (U-NII) Bands"* [Online]. Available: `https://transition.fcc.gov/oet/ea/presentations/files/may17/31-Part-15-Panel-UNII-UpdatesDT.pdf` Accessed Jan 2019.

[55] FCC, *"CFR 47 Part 15 Subpart E"*, [Online]. Available: https://www.ecfr.gov/ Accessed Jan 2019.

[56] Erik Dahlman, Stefan Parkvall, Johan Skold *"4G, LTE-Advanced Pro and The Road to 5G"*. Academic Press; 3 edition (July 19, 2016)

[57] Perahia, Eldad and Robert Stacey, *"Next Generation Wirelss LANs - Throughput, Robustness and Reliability in 802.11n"*. Cambridge University Press, 2008.

[58] Cisco Systems, *"Voice over Wireless LAN 4.1 Design Guide, Cisco Validated Design I"*. Cisco Systems, Inc. January 18, 2010.

[59] LTE-U Forum, *"LTE-U SDL coexistence specifications version 1.3"* [Online]. Available: `https://web.archive.org/web/20170303112953/http://lteuforum.org/uploads/3/5/6/8/3568127/lte-u_forum_lte-u_sdl_coexistence_specifications_v1.3.pdf` Accessed May 2018.

[60] Qualcomm Technologies, Inc., *"Qualcomm research LTE in unlicensed spectrum: harmonious coexistence with Wi-Fi."* [Online]. Available: https://www.qualcomm.com/media/documents/files/lte-unlicensed-coexistence-whitepaper.pdf

[61] A. K. Sadek, *"Carrier sense adaptive transmission (CSAT) in unlicensed spectrum,"* 2014. US Patent App. 14/486,855.

[62] Multi-node tests for Licence-Assisted Access (LAA), 3GPP TR 36.789 V13.0.0 (2017-06).

[63] Evolved Universal Terrestrial Radio Access (E-UTRA) and Evolved Universal Terrestrial Radio Access Network (E-UTRAN); Overall description, 3GPP TS 36.300 V13.8.0 (2017-06).

[64] Physical channels and modulation, 3GPP TS 36.211 V13.6.0 (2017-06).

[65] Base Station (BS) radio transmission and reception, 3GPP TS 36.104 V13.8.0 (2017-06).

[66] Base Station (BS) conformance testing, 3GPP TS 36.141 V13.8.0 (2017-06).

[67] Requirements for support of radio resource management, 3GPP TS 36.133 V13.8.0 (2017-06).

[68] https://en.wikipedia.org/wiki/QoS_Class_Identifier

[69] Intel Whitepaper, *"LTE-WLAN Aggregation (LWA): Benefits and Deployment Considerations,"* [Online]. Available: https://www.intel.com/content/www/us/en/wireless-network/lte-wlan-aggregation-deployment-white-paper.html. Accessed May 2018.

[70] Qualcomm Whitepaper, *"Making the Best Use of Unlicensed Spectrum,"* [Online]. Available: https://www.qualcomm.com/documents/making-best-use-unlicensed-spectrum-presentation. Accessed May 2018.

[71] Multefire Alliance, "About the MulteFire Release 1.0 Specification," [Online]. Available: https://www.multefire.org/specification/. Accessed May 2018.

[72] Multefire Alliance, *"MulteFire Release 1.0 Technical Paper A New Way to Wireless*, [Online]. Available: https://www.multefire.org/wp-content/uploads/MulteFire-Release-1.0-whitepaper_FINAL.pdf. Accessed May 2018.

[73] Multefire Alliance, *"MulteFire Release 1.0.1*, [Online]. Available: https://www.multefire.org/specification/specification-release-1-0-1download/. Accessed May 2018.

[74] G. Bianchi, *"Performance Analysis of the IEEE 802.11 Distributed Coordination Function,"*. IEEE Journal on Selected Areas in Communications vol. 18, no. 3, pp. 535-547, Mar. 2000

[75] M. Ergen and P. Varaiya, *"Throughput analysis and admission control for ieee 802.11 a,"*. Mobile networks and Applications, vol. 10, no. 5, pp. 705–716, 2005.

Appendix A

Abbreviations

3GPP ..... 3rd Generation Partnership Project

AC ..... Access Category

ACK ..... Acknowledgment

AIFS ..... Arbitration Inter-Frame Spacing

AP ..... Access Point

BER ..... Bit Error Rate

BS ..... Base Station

CAPC ..... Channel Access Priority Class

CCA ..... Clear Channel Assessment

CFP ..... Contention Free Period

CF-Poll ..... Contention Free Poll

CFR ..... Code of Federal Regulations

COT ..... Channel Occupancy Time

CP ..... Contention Period

CSAT ..... Carrier Sense Adaptive Transmission

CSMA/CA ... Carrier Sensing Multiple Access Collision Avoidance

CTS ..... Clear-to-Send

CW ..... Contention Window

DCF ..... Distributed Coordinated Function

DCS ..... Dynamic Channel Selection

DL ..... Downlink

DTX ..... Discontinuous Transmission

ECCA ..... Extended Clear Channel Assessment

EIRP ..... Equivalent Isotropically Radiated Power

eLAA ..... Enhanced License Assisted Access

eNB ..... Evolved Node B

EPC ..... Evolved Packet Core

E-UTRA ..... Evolved Universal Terrestrial Radio Access

E-UTRAN .... Evolved Universal Terrestrial Radio Access Network

FCC ..... Federal Communications Commission

HARQ ..... Hybrid Automatic Repeat Request

HCCA ..... HCF Controlled Channel Access

HCF ..... Hybrid Coordination Function

IEEE ..... Institute of Electrical and Electronics Engineers

IoT ..... Internet of Things

IP ..... Idle Period

IPR ..... Internet Protocol

ISM ..... Industrial Scientific and Medical

ITU ..... International Telecommunication Union

ITU-D ..... ITU Telecommunication Development Sector

ITU-R ..... ITU Radiocommunication Sector

ITU-T ..... ITU Telecommunication Standardization Sector

LAA ..... License Assisted Access

LBT ..... Listen Before Talk

LTE ..... Long Term Evolution

LTE-U ..... LTE Unlicensed

LWA ..... Long Term Evolution Wireless Local Area Network Aggregation

MAC ..... Medium Access Control

MCOT ..... Maximum Channel Occupancy Time

MCS ..... Modulation and Coding Schemes

MNO ..... Mobile Network Operator

NACK ..... Negative Acknowledgment

NHN ..... Neutral Host Network

NTIA ..... National Telecommunications and Information Administration

OFDMA ..... Orthogonal Frequency Division Multiple Access

PDCCH ..... Physical Downlink Control Channel

PDCP ..... Packet Data Convergence Protocol

PDSCH ..... Physical Downlink Shared Channel

PHY ..... Physical Layer

QCI ..... QoS Class Indicator

QoS ..... Quality of Service

RAN ..... Radio Access Network

RRM ..... Radio Resource Management

RS ..... Reference Signal

RTS ..... Request-to-Send

SCell ..... Secondary Cell

SDL ..... Supplemental Downlink

TDM ..... Time Division Multiplexing

TS ..... Technical Specification

TxOP ..... Transmission Opportunity

UE ..... User Equipment

UL ..... Uplink

U-LTE ..... Unlicensed Long Term Evolution

UN ..... United Nations

U-NII ..... Unlicensed National Information Infrastructure

US ..... United States

WLAN ..... Wireless Local Area Network